A COMPARATIVE MICROSCOPIC STUDY OF HUMAN AND NON-HUMAN LONG BONE HISTOLOGY

Faridah Mohd NOR

submitted for the degree
of Doctor of Philosophy

Department of Archaeological Sciences

University of Bradford

2009

Abstract

Identification of human or nonhuman skeletal remains is important in assisting the police and law enforcement officers for the investigation of forensic cases. Identification of bone can be difficult, especially in fragmented remains. It has been reported that 25 to 30% of medicolegal cases, which involved nonhuman skeletal remains have been mistaken for human. In such cases, histomorphometric method was used to identify human and nonhuman skeletal remains. However, literature has shown that histomorphometric data for human and nonhuman bone were insufficient. Additionally, age estimation in bone may help in the identification of human individual, which can be done by using a histomorphometric method. Age estimation is based on bone remodeling process, where microstructural parameters have strong correlations with age. Literature showed that age estimation has been done on the American and European populations. However, little work has been done in the Asian population. The aims of this project were thus, to identify human and nonhuman bone, and to estimate age in human bones by using histomorphometric analysis. In this project, 64 human bones and 65 animal bones were collected from the mortuary of the Universiti Kebangsaan Malaysia Medical Centre and the Zoos in Malaysia, respectively. A standard bone preparation was used to prepare human and nonhuman bone thin sections for histomorphometric assessment. Assessments were made on the microstructural parameters such as cortical thickness, medullary cavity diameter, osteon count, osteon diameter, osteon area, osteon perimeter, Haversian canal diameter, Haversian canal area, Haversian canal perimeter, and Haversian lamella count per osteon by using image analysis, and viewed under a transmitted light microscope. The

microstructural measurements showed significant differences between human and nonhuman samples. The discriminant functions showed correct classification rates for 81.4% of cases, and the accuracy of identification was 96.9% for human and 66.2% for animal. Human age estimation showed a standard error of estimate of 10.41 years, comparable with those in the literature. This study project offers distinct advantages over currently available histomorphometric methods for human and nonhuman identification and human age estimation. This will have significant implications in the assessment of fragmentary skeletal and forensic population samples for identification purposes.

Keywords: Histomorphometric method; Haversian canal area; cortical thickness; image analysis; human.

Supervisors: Holger Schutkowski and Jo Buckberry.

TABLE OF CONTENTS

List of Figures

List of Tables

List of Abbreviations

CT: Cortical thickness

HCA: Haversian canal area

HC: Haversian canal

HCD: Haversian canal diameter

HCP: Haversian canal perimeter

HLC: Haversian lamellae count

Log : Logarithm

MCD: Medullary cavity diameter

n: Total number

OC: Osteon count

OD: Osteon diameter

OP: Osteon perimeter

SD: Standard deviation

SEE: Standard error of estimate

Acknowledgements

My gratitude goes to my supervisor, Robert F. Pastor who has given full support, advice, encouragement and inspiration to this project. My appreciation also goes to Holger Schutkowski who has assisted me throughout the experimentation of this project. I am grateful to Ben Stern and Belinda Bottomley from University of Bradford who have helped me in setting up some of the laboratory equipment, and ensured the smooth running of my sample preparation in the chemistry laboratory. My thanks go to David Jerwood, University of Bradford who provided me the statistical assistance throughout the thesis. My special thanks go to Universiti Kebangsaan Malaysia (UKM) who has been willing to fund this project.

I would like to express my sincere gratitude to Encik Abdul Rahman Mohd Isa, Encik Mohd Rahim and Encik Mohd Taha from the Universiti Kebangsaan Malaysia, who have assisted me in the data collection, staff from Zoo Negara Malaysia and Zoo Melaka, as well as, Dr Kevin Lazarus from Zoo Taiping for providing me the access to the animal skeletal remains. Finally, thanks to my husband, Zaid Muda for his moral support, and to my children for behaving well throughout the writing of this thesis. I would also like to thank my parents, Mohd Nor Jaafar and Saliah Jantan for their moral support throughout the whole duration of my studies.

1. INTRODUCTION

Identification of human and nonhuman skeletal remains is vital in assisting the police and law enforcement officers in the investigation of medicolegal cases. Identification of human or nonhuman bone can be difficult in fragmented remains, and in such cases a histomorphometric method may be useful. In this study, identification of human and nonhuman bone and age estimation in human will be done by using a histomorphometric method.

Bone is a mineralised connective tissue, which harbours bone marrow, where blood cells are formed. Bone supports and protects the internal organs such as brain, lungs and heart; and forms a system of levers to assist in skeletal muscle contraction and bodily movements (Junqueira and Carneiro, 2005; Wheater and Burkitt, 1987). Additionally, it provides a source of inorganic ions mainly, calcium and phosphate to the body.

1.1 Histological structure of human and nonhuman bones

Generally, both human and nonhuman bones have a similar basic histological structure (Geneser, 1986; Miller *et al*., 1964; Torrey and Feduccia, 1979; Welsch and Storch, 1976). Bone comprises three types of bone lining cells, namely osteoblasts, osteocytes and osteoclasts, which are present in the intercellular matrix of calcified material (Geneser, 1986). Bone is covered by periosteum on the external surface, and endosteum on the internal surface.

1.1.1 Bone lining cells

1.1.1.1 Osteoblast

An osteoblast is a bone-forming cell, which synthesises and secretes bone matrix. Osteoblasts form like aggregations comprising an epithelium of low columnar cells. The cytoplasm contains significant amounts of alkaline phosphatase, and the the cells remain in contact with each other through short, slender processes (Geneser, 1986). Osteoblasts are responsible for the synthesis of type I collagen, proteoglycans and glycoproteins. The newly-formed organic matrix is known as an osteoid, and it becomes calcified almost immediately after deposition in a developing bone (Wheater and Burkitt, 1987). When bone formation ceases, the osteoblasts return to the osteoprogenitor stage so that the amount of alkaline phosphatase in the cytoplasm decreases (Geneser, 1986).

The differentiation pathway can be varied for osteoblasts. The stromal stem cell for an osteoblast is pluripotential, and it can differentiate into either osteoblast or osteoclast precursor cell lineage, and form osteoblasts and osteoclasts, respectively (Figure 1) (Raisz, 1999). The mesenchymal stem cells or stromal stem cells can also differentiate into adipocytes or marrow support cells, and into fibroblasts, muscle cells or cartilage cells (Figure 2). The pathway to adipocytes is of particular importance because cells that are diverted into this lineage are no longer available for bone formation. This may account for the fact that as marrow becomes fatty with aging, osteoblast renewal may be impaired.

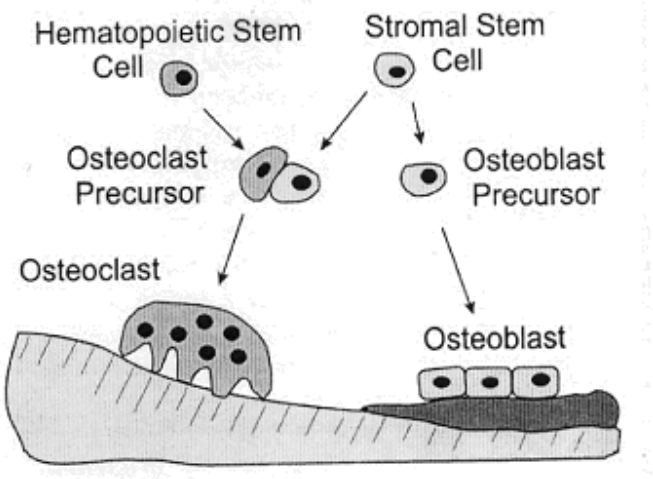

Figure 1 Interaction of hematopoeitic and stromal cells to produce osteoclast and osteoblast cell, respectively (from Raisz, 1999).

Once the osteoblast has differentiated and completed its cycle of matrix synthesis, it becomes a flattened lining cell on the bone surface and is buried in the bone as an osteocyte, or undergoes programmed cell death (apoptosis) (Figure 2). The osteocytes are critical for maintaining fluid flow through the bone, and changes in this fluid flow provide signals for cellular response to mechanical forces.

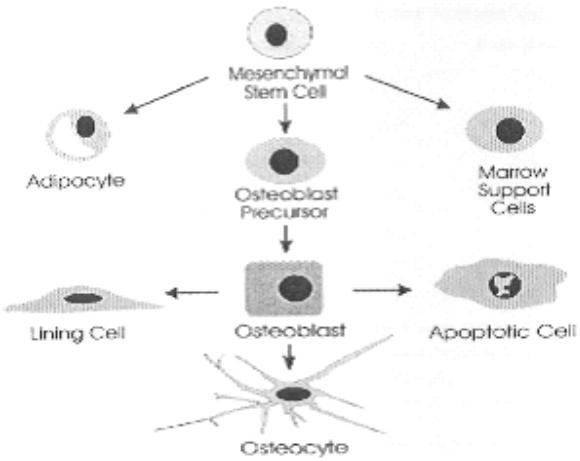

Figure 2 Origin and fate of osteoblast (from Raisz, 1999).
This figure denotes the multiple pathways of mesenchymal stem cell to become either adipocyte, osteoblast or marrow cells.

1.1.1.2 Osteocyte

Osteocytes form the chief cellular component of mature bone. During bone formation, osteocytes are formed from resting osteoblasts, which are incorporated into small spaces called lacunae in the matrix. Osteocytes possess numerous canaliculi consisting of cytoplasmic processes, which anastomose with canaliculi from adjacent cells (Junqueira and Carneiro, 2005) for the exchange of tissue fluids and metabolites between the osteocytes and blood capillaries.

An osteocyte has organelles, which produce matrix constituents throughout life (Cormack, 1987). An osteocyte releases calcium ions from the bone matrix when calcium demands increase. It is capable of transferring calcium ions from bone mineral to blood in a process called osteocytic osteolysis (Geneser, 1986). The osteolysis process is controlled by interactions between parathyroid hormone and calcitonin, whereby parathyroid hormone stimulates the osteolysis, and calcitonin inhibits it.

1.1.1.3 Osteoclast

Osteoclast is a motile, large multinucleated cell with numerous vacuoles and lysosomes in the cytoplasm, which is also known as a bone-resorbing cell in bone remodeling process (section 1.2). An osteoclast is formed from the fusion of monocyte and macrophage, and is found on a resorbing surface known as Howship's lacuna, which is created by enzymatic digestion from the osteoclast. During the resorption process, part of the osteoclast will become deeply infolded known as the 'ruffled border' (Cormack, 1987; Junqueira and Carneiro, 2005; Shipman *et al*., 1985) (Figure 3). The ruffled border consists of branching, motile finger-like processes, which pierce through the bone surface. Large vacuoles filled with lysosomal enzymes in the osteoclast will move toward

the ruffled border, and release enzymes to digest bone (Cormack, 1987; Junqueira and Carneiro, 2005; Shipman et al., 1985; Wheater and Burkitt, 1987). Organic acids such as carbonic, citric and lactic acids are excreted into the bone matrix to bring about focal decalcification. Apatite and collagen digested from the bone will then move into the ruffled border, and pinch off to form vesicles in the osteoclast, which will be transferred to blood capillaries (Figure 3).

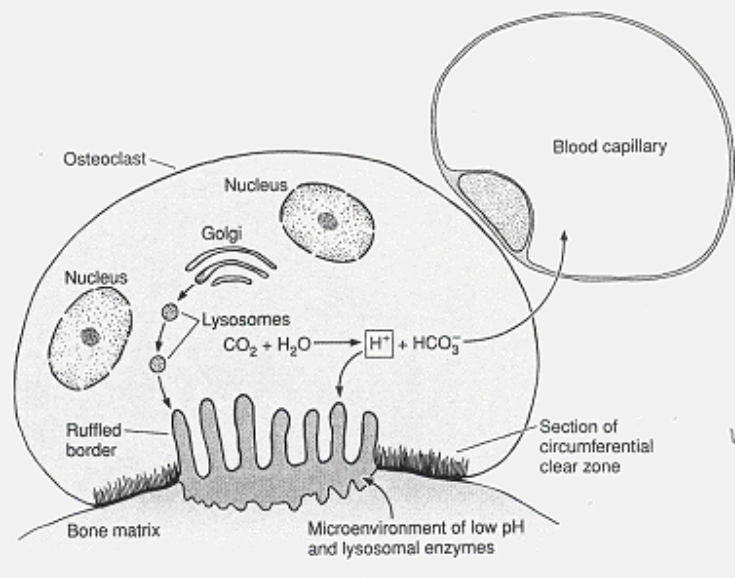

Figure 3 Bone resorption process (from Junqueira, 2005: p. 137).
This figure illustrates the osteoclast attachment to bone surface with the formation of a 'ruffled border' to digest bone matrix, and to remove the products to cytoplasm and blood capillaries.

Osteoclast activity is controlled by hormones such as calcitonin and parathyroid hormones, and by small signalling proteins known as cytokines. Calcitonin, which is produced by the thyroid gland, inhibits the osteoclasts activity by inhibiting bone resorption. Parathyroid hormone stimulates the osteoclasts activity through the production of osteoclast stimulating factor (Junqueira and Carneiro, 2005).

1.1.2 Bone matrix

Th intercellular bone matrix comprises organic and inorganic componens. About 90% of its organic content is contributed by the presence of collagen, and the remaining 10% is contributed by the amorphous component of ground substance. The inorganic matter is comprised of hydroxyapatite mineral, which contributes to 70% of its dry weight (Cormack, 1987). The presence of abundant collagen in bone matrix contributes to its significant strength and flexibility. Collagen is a structural protein, which is found in most connective tissues such as tendons, ligaments and skin. Most of the collagen in bone matrix is type I collagen and small quantities of type V collagen. The presence of collagen provides loci for calcium and phosphate mineralisation.

The ground substance comprises glycoproteins, sialoproteins, proteoglycans and noncollagenous proteins. The glycoproteins are mainly chondroitin sulphate and hyaluronic acid. Noncollagenous proteins include osteocalcin, osteopontin and osteonectin. Osteocalcin is secreted by osteoblasts, and is the most abundant protein in bone. Osteocalcin is important in bone mineralisation, and serves as a chemo-attractant for bone cells. Osteonectin serves to bind collagen to minerals in the bone matrix, while osteopontin determines the binding between bone minerals and cells (Martin *et al*., 1998). Bone minerals comprise calcium and phosphate in the form of hydroxyapatite crystals, $Ca_5 (PO_4)_3(OH)$. The crystals are in the form of slender rods or plates with hexagonal symmetry (Weiner and Traub, 1991). The combined action of collagen and glycosaminoglycans facilitates the precipitation of calcium phosphate (Geneser, 1986). Once crystallisation has formed, it will grow and catalyse further crystallisation. Crystals of hydroxyapatite can also combine with matrix vesicles, giving rise to rounded

outgrowths from osteoblasts. The vesicles consist of enzymes, which act as calcification initiators and provide a suitable environment for hydoxyapatite deposition. The crystals and lamellae are arranged parallel to each other, with dissimilar crystal arrangements in each lamella. Other ions such as magnesium, potassium, sodium, carbonate and citrate ions are present in non-crystalline forms on the surface of the apatite crystals so that they form as ion substitution with the crystal lattice. Additionally, there is a layer of water and ions surrounding the crystal known as hydration shell to facilitate the exchange of ions between the crystal and body fluids.

1.1.3 Periosteum and endosteum

The principle functions of periosteum and endosteum are to provide new osteoblasts for repair and growth of bone and a continuous supply of nutrition. The periosteum consists of two layers; that is an outer fibrous layer and an inner osteogenic layer (Ham and Cormack, 1979; Welsch and Storch, 1976). The outer layer of periosteum has large blood vessels and consists of collagenic fibres, elastic fibres and fibroblasts. The periosteum has Sharpey's fibres to form as anchors to the bone surface (Figure 4). Cells of the osteogenic layer are important as they can transform into bone lining cells. The endosteum lines the spaces in marrow cavity and Haversian canals of compact bone. The endosteum consists of connective tissue and flattened osteoprogenitor cells. The osteoprogenitor cells can be transformed into osteoblasts, particularly during bone growth and repair (Ham and Cormack, 1979; Junqueira and Carneiro, 2005).

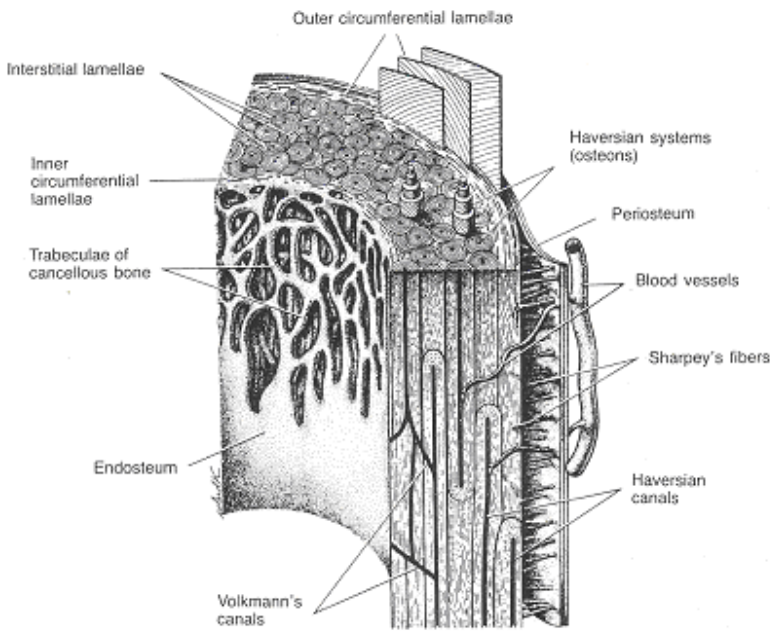

Figure 4 A diagrammatic representation of a compact long bone in cross section and longitudinal section (From Geneser, 1986: p. 229).
This figure illustrates numerous blood vessels in the periosteum, and the Sharpey's fibres which anchor the periosteum to the bone surface.

1.1.4 Types of bone

Macroscopic examination of bone in cross section of bone can be divided into compact and cancellous bone. Compact bone is located on the outer aspect of the bone, and shows a dense area without cavities, whereas cancellous bone is the inner aspect of bone, which shows numerous interconnecting cavities. Microscopic examination of both compact and cancellous bones shows the same basic histological structures (Junqueira and Carneiro, 2005). Compact bone may be classified as primary or secondary bone.

1.1.4.1 Primary bone

Primary bone is the first bone to appear in fracture repair and other repair processes. It is characterised by the random deposition of fine collagen fibres. Primary bone is laid down in an existing bone surface such as the periosteum during growth. Primary bone may be

further subdivided into primary circumferential lamellar bone and plexiform bone (Martin *et al*., 1998).

Primary circumferential lamellae bone

Primary circumferential lamellar bone shows lamellae arranged parallel to the bone surface. Primary osteons are formed when blood vessels are incorporated into the lamellar structure so that each vessel is surrounded by several concentric lamellae (Figure 5). A primary osteon has a central canal consisting of blood vessels, nerves and loose connective tissue. A primary osteon has no cement line surrounding it, compared to secondary osteon (Figure 5), which have a distinct cement line.

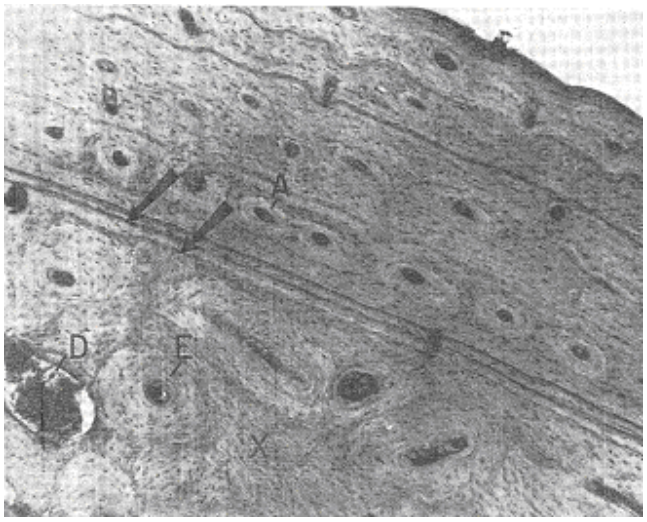

Figure 5 A femoral section of a rhesus monkey (100x magnifications) in a decalcified and stained bone preparation (from Enlow 1963: p. 64).
The figure shows primary osteon (marked 'A'), Haversian system (marked 'E') and resorption space (marked 'D').

Plexiform bone

Plexiform bone comprises a mixture of trabecular structures and lamellar bone. Plexiform bone is formed by a continuous production of a trabecular network, which is filled in by lamellar bone. In the formation of this bone, the lamination of vascular canals occurs, but

the vessels of one layer are connected with adjacent layers of vessels by numerous, short, radial canals. They form a symmetrical, three-dimensional plexus of primary canals with vascular spaces in a horizontal, rectangular shape giving its 'brick wall' appearance (Figure 6). It may form from both sub-periosteal deposition and endosteal deposition. The rate of formation of plexiform bone is faster than the primary circumferential lamellar bone. Plexiform bone is found in large, fast-growing animals such as cattle, deer, pigs, young monkeys and humans (Martin and Burr, 1989).

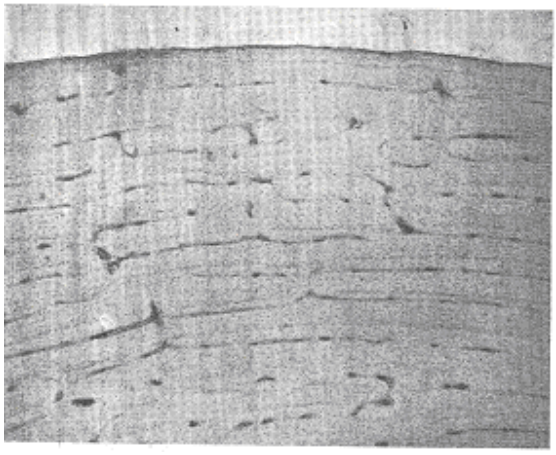

Figure 6 Plexiform bone pattern (from Enlow, 1963: p. 66).
The figure shows plexiform bone pattern in a femur mid-diaphyseal section of a dog (60x magnifications) in a decalcified and stained bone preparation.

1.1.4.2 Secondary bone

Secondary bone tissue comprises lamellae arranged parallel to each other, and the lamellae are arranged in concentric form around vascular canals, also known as Haversian systems or osteons (Junqueira and Carneiro, 2005). Haversian systems are found in humans and large animals. Haversian systems are formed when a group of four to twenty concentric lamellae surround a central Haversian canal (Figure 5). The deposition of lamellae starts from the periphery moving centrally, so that the most

recently formed lamella is lying close to the central canal (Junqueira and Carneiro, 2005). Older Haversian systems tend to have smaller canals, while younger systems have larger canals.

In longitudinal section, each Haversian system is a long, bifurcated cylinder, lying parallel to the long axis of the diaphysis (Figure 4). The Haversian systems form the central part of a long bone. They are supported by layers of interstitial lamellae, which are present between the Haversian systems and also by outer circumferential lamellae beneath the periosteum and inner circumferential lamellae on the endosteum. Volkmann's canals (Figure 4) are transverse canals, which are interconnected with the longitudinal Haversian canals, the marrow cavity, and the periosteum.Volkmann's canals are not surrounded by concentric lamellae, as they traverse transversely and obliquely to the long axis of the bone. Haversian canals, Volkmann's canals (Wachter *et al*., 2002) and lacunar-canaliculi (Weinbaum *et al*., 1994) are porous structures in cortical bone.

1.2 The bone remodelling process

The bone remodelling cycle involves a series of highly regulated steps that depend on the interactions between the two cell lineages namely, the mesenchymal osteoblastic lineage and haematopoeitic osteoclastic lineage (Raisz, 1999). Remodelling in the osteon, periosteum and endosteum is accomplished by teams of osteoclasts and osteoblasts that work simultaneously in basic multicellular units (*BMUs*) (Martin *et al*., 1998; Robling and Stout, 1999b). Bone remodelling occurs in multiple locations of the skeleton (Junqueira and Carneiro, 2005) to remove older bone and replace it with newly-formed bone. Osteon remodelling forms a Haversian system, known as a bone structural unit (*BSU*) (Marieb, 2001), while remodelling in the endosteum and periosteum causes

thinning of the periosteum, as formation exceeds resorption on the periosteal surface and resorption exceeds formation on the medullary canal.

1.2.1 The cellular basis of bone remodelling

The cellular basis of bone remodelling has been described by Parfitt (1984) in the 'quantum concept'. The 'quantum concept' explains bone remodelling process at the cellular level, which ultimately forms *BSU* or Haversian systems. In this concept, the bone remodelling process can be defined in five stages namely, quiescence, activation, resorption, reversal, formation (Parfitt, 1984). In a normal state, 80% of bone surfaces are in the quiescent stage. Activation of remodeling process requires the recruitment of osteoclasts and mononuclear cells into the connective tissue, which leads to migration and fusion of large multinucleated osteoclasts.

The intracortical *BMU* has two basic units, comprising a cutting cone, preosteoblast and osteoblast-lined closing cone (Ham and Cormack, 1979; Robling and Stout, 1999a) (Figure 7). A cutting cone, which occurs from a pre-existing primary osteon, is usually lined with mononuclear cells and osteoclasts. Mononuclear cells release an osteoclast-stimulating agent called prostaglandin. These cells are attached to the mineralised bone surface, and initiate resorption by secreting hydrogen ions and lysosomal enzymes, particularly cathepsin *K*, which degrades all components of bone matrix including collagen. Osteoclastic resorption produces either an irregular scalloped cavity on the trabecular bone surface called Howship's lacunae or on the Haversian canal in cortical bone.

On completion of the resorption stage, there is a reversal phase during which mononuclear cells are seen on the bone surface. They involve in further degradation of

collagen to initiate the formation phase. During the formation phase, the cavity created by resorption is completely filled in by successive layers of osteoblasts and deposits a mineralisable matrix. Osteocytes and bone lining cells help to terminate the activities in the resorption cavities by releasing prostacyclin. The preosteoblast and osteoblast-lined closing cone is responsible for the deposition of lamellar layers on the walls of the resorptive bay (Eriksen and Langdahl, 1995). As each *BMU* advances through or across the bone surface, it creates and leaves behind successive cycles of resorption followed by formation; each cycle represents the balance between resorbed old bone and formation of new bone.

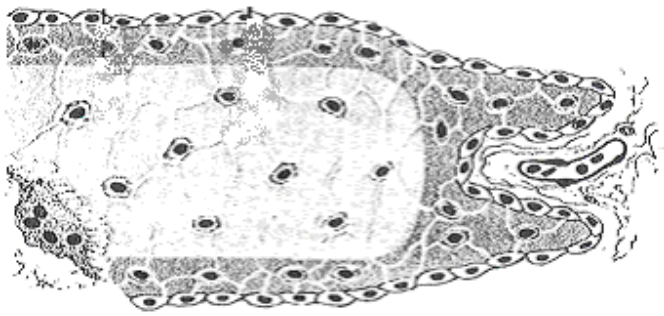

Figure 7 Bone remodelling unit (*BMU*) (from Ham and Cormack, 1979: p. 383)
The longitudinal section of a *BMU* tunnelling to the right with osteoclasts on the resorbing surface (lower left corner) and capillary on the right to supply nutrients to the cells. The *BMU* is covered with a layer of osteogenic cells, which differentiate into osteoblasts, and form a new layer of bone by secreting organic intercellular matrix, present on the left in the refilling surface.

Each *BMU* creates a temporary deficit of bone, which constitutes the remodelling space. The remodelling space is created by the lapse of time taken for bone resorption and formation to complete their activities. Bone formation commences several weeks after resorption is completed, after which several months will elapse before the bone replacement process is completed. The volume of remodeling space is proportional to the

rate of bone remodelling, so that the space expands when remodelling increases and contracts when remodelling decreases.

1.3 Control of the remodelling process

1.3.1 Hormonal control

Systemic regulators of bone remodelling

The remodelling process can be triggered by changes in calcium and phosphorus blood levels (Raisz, 1999). The metabolic functions of the skeleton are served by parathyroid hormone (*PTH),* a calcium-regulating hormone. Calcium homeostasis is regulated by interactions between calcitonin (*CT*) and parathyroid hormone (*PTH*) (Marieb, 2001) through actions on osteoblasts and osteoclasts, respectively (Carter and Schipani, 2006).

When calcium blood level rises, *CT* is released by parafollicular cells of the thyroid gland. Calcitonin inhibits bone resorption, and stimulates calcium salt deposition in bone matrix, and thus reduces blood calcium levels. When calcium blood level declines, *PTH* is released by the parathyroid gland, which stimulates osteoclasts to resorb bone, and thus releases calcium to the blood. As blood concentration of calcium rises, the stimulus for *PTH* release will cease.

Plasma *PTH* regulates serum calcium concentration. It is a potent stimulator of bone resorption, and has biphasic effects on bone formation. There is an acute inhibition of collagen synthesis with a high concentration of this hormone, but prolonged exposure to intermittent level of this hormone produces increased bone formation. Plasma *PTH* tends to increase with age, which may produce an increase in bone remodelling activity, and thus a loss of cortical bone.

The most important systemic hormone in maintaining normal bone remodelling is oestrogen. In menopausal women, as oestrogen becomes deficient, more osteoclasts are recruited for bone remodelling, and a few osteoblasts are recruited to refill each cavity. Oestrogen also stimulates an increased local production of interleukin-6 and other cytokines for the bone remodelling process (Parfitt, 1996).

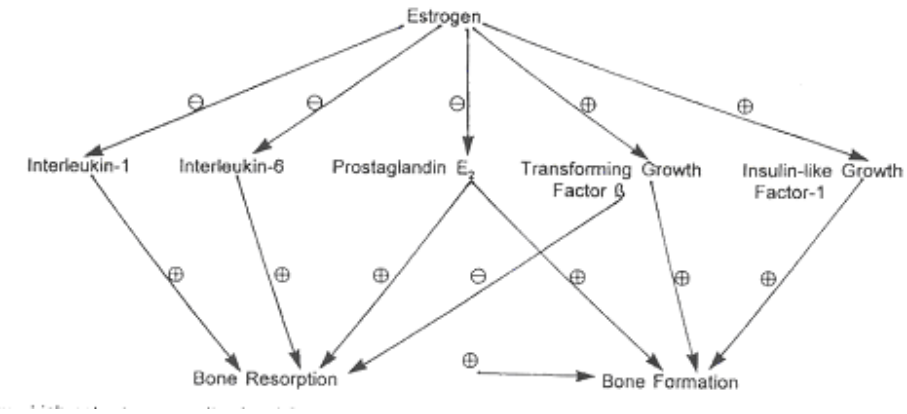

Figure 8 Pathways by which oestrogen interacts with local factors to influence bone remodelling (from Raisz, 1999).
This figure shows interactions of oestrogen with interleukins, prostaglandin and growth factors to influence bone remodelling.

1.3.2 Response to mechanical stress

The bone remodelling process can be triggered by changes in mechanical forces or microdamage (Turner, 1998). Wolff's law states that when there are forces acting on the bone, the bone will respond by undergoing remodelling (Frost, 1990; Marieb, 2001). When weight exerts some stress on the bone, it tends to bend the bone. The bending forces tend to compress the bone on one side compared to tension forces, which stretch the bone on the other side (Figure 9). Both forces become minimal toward the centre of the bone, and tend to be absorbed by the spongy bone (Frost, 1990; Marieb, 2001).

Wolff's area law explains further that bending stresses are the greatest at the midshafts of long bones, where they are the thickest. Similarly, curved bones will buckle at the thickest site. Bending stresses become minimal toward the thickest part of curved and long bones, as in the midshafts of long bones, where the forces tend to be absorbed by the spongy bone. The trabeculae of spongy bone will undergo compression by forming struts or lines of forces along the lines of trabeculae. Finally, heavy muscle attachment occurs at large bony projections (Frost, 1990; Marieb, 2001), which explains the radial expansion in endosteal and periosteal surfaces in the remodelling process due to heavy muscle attachments.

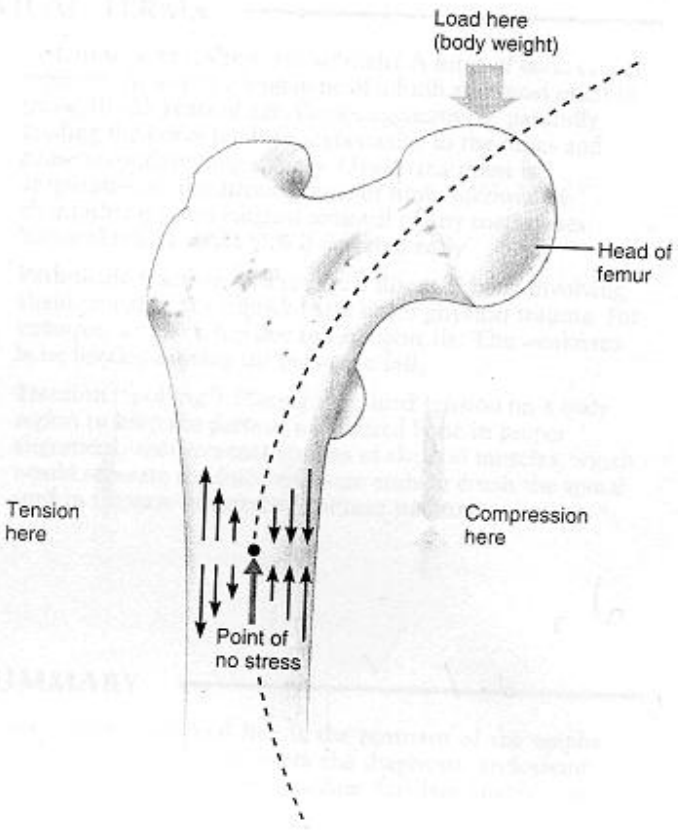

Figure 9 The bone anatomy and lines of stress (From Marieb, 2001: p. 187).
The arrow indicates the lines of stress exerted on a bone. When the load is transmitted to the head of the femur, the bending of the bone will occur along the indicated arc. The

bending compresses the bone on one side (converging arrows), and stretches the bone on the other side (diverging arrows). The forces cancel each other internally, so that less bone is needed internally than externally.

1.4 Identification of human and nonhuman bones

The police, forensic anthropologists and law enforcement officials are being required to identify fragmented skeletal remains, as their involvement in forensic situation expands. Retrospective analysis of medicolegal cases showed that 15 to 25% cases of nonhuman skeletal remains have been mistaken for human (Owsley and Mann, 1990). In the forensic setting, skeletal remains are often fragmented due to exposure to weather, predator bites (Murad and Boddy, 1987), altered by weaponry and degraded or burned (Cattaneo *et al*., 1999; Thompson, 1999). Identification of human and nonhuman (animal) bone in such cases may be done by macroscopic and microscopic methods.

1.4.1 Macroscopic method

The macroscopic analysis of bear paws and human feet have shown morphologic differences, which can be used to identify human and animal (Gilbert, 1980). Gilbert (1980) has shown that in bear paws, the navicular and lunar bones are united, compared to human feet, whereby the navicular and lunar bones occur separately. In terms of size, the pisiform bone in bear paws is larger than in human hands. Additionally, cortical bone thickness may be used to identify human and animal. When viewed in cross-section, the cortex of an adult human bone is one-fourth the total diameter, whereas in large mammals such as dog or bear, the cortex is much thicker that is, one-third the total diameter (Figure 10). In contrast, birds have very thin bones, which is only one-eighth the total diameter of the bone (Thomas, 1995). However, in severely fragmented skeletal

remains, the macroscopic method may not be feasible, and other methods of identification may be required to identify human or nonhuman.

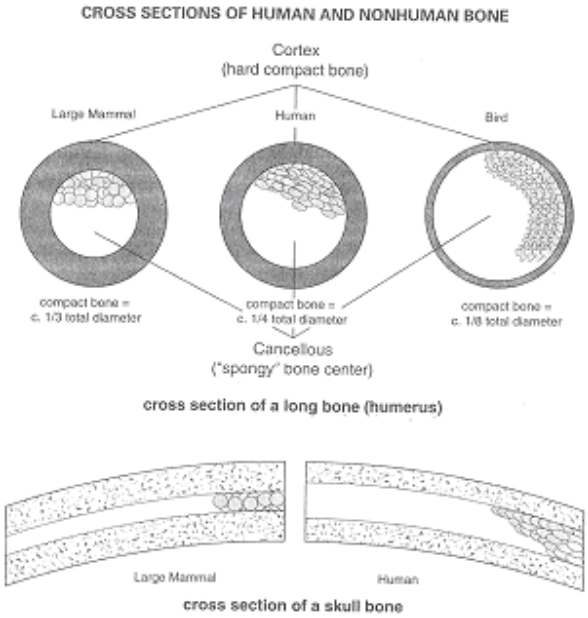

Figure 10 Cortical thickness in large mammal, human and bird (From Thomas, 1995: p. 18).
The figure shows the cortical thickness in large mammal, human and bird in descending order of thickness.

1.4.2 Microscopic method

Microscopic method has been useful in the identification of human and nonhuman bone, especially in fragmented skeletal remains (Enlow and Brown, 1956; Enlow and Brown, 1957; Enlow and Brown, 1958). Microscopic analyses in fossil and recent mammalian bones have provided good references for different types of animals, from the lowest to the highest vertebrate groups, based on their histologic patterns (Enlow and Brown, 1956; Enlow and Brown, 1957; Enlow and Brown, 1958). Rabbit bone has a mixture of primary canals, secondary canals and Haversian systems. Primary canals are present in most part of the compact bone, and each primary canal is surrounded by one, two or three rings of

osteocytes forming a Haversian-like structure. These primary vessels occupy a greater portion of the compact bone without Haversian system, or areas of dense Haversian system may occur. The ribs and skull bones are largely Haversian systems, and well-developed Haversian systems appear in several generations. In very dense Haversian tissues, secondary osteons of second, third and even fourth generations are superimposed on each other in older tissue areas. The thin compact bone found in the vertebral processes is composed of a primary, reticular tissue containing scattered Haversian systems. Primary, reticular tissue is deposited as a series of lamellae, which enclose a number of small primary vascular canals with no specific arrangement of the vessels with regards to lamella or osteon. This primary bone pattern is mostly found in outer or periosteal bone regions.

In the mandible and maxilla bones of a cat, dense Haversian systems are present. The outer circumferential lamellar layer is narrow. The endosteal layer is usually thick and well-developed. Volkmann's canals are frequently seen. In areas that are deficient in vascularisation, irregular Haversian systems are separated by large interstitial lamellar areas. The long bones follow the same pattern of inner and outer circumferential lamellation, enclosing a middle compact bone, composed of Haversian systems. In the epiphysis of long bones, there are mainly primary bones in the middle of compact bone with scattered Haversian systems.

The compact bone of a lion is similar to that of a domestic cat, but it is considerably larger. The outer lamellae layer is relatively thin, and contains small primary canals that eventually become Haversian systems. The middle secondary region is broad and filled with dense Haversian systems.

The mandibular bone of a squirrel is composed of primary radial canals (in radial rows), which penetrate the compact bone both from endosteal and periosteal borders, with limited areas of longitudinal canals (in longitudinal direction).

The long bones of animals such as hog, cow and goat have a well-organised plexiform bone pattern. The outer portions of the compact bone are usually composed exclusively of plexiform bone consisting of primary canals. In older tissue regions, few scattered Haversian systems are developing. The endosteum often consists of dense Haversian system. In the diaphysis of long bones, vascular arrangement is reticular, and extensive Haversian system is present.

The antler of a deer is composed of a very broad compact bone encircling the inner spongy tissue. The vessels follow a complex reticular or plexiform pattern, and some appear to have Haversian system. Both plexiform and reticular tissues have the same basic pattern, but they are different in that, reticular bone tissue has unorganised vascular canals, which may extend and branch in almost any direction, compared to plexiform bone, which has organised vascular canals. The rib tissues of the cow and the goat are composed of dense Haversian system, but in the domestic hog, the bone has remained entirely plexiform.

The long bones of a horse vary in tissue structure according to location. In the diaphysis, the basic primary vascular pattern is reticular. In diaphysis, the basic primary vascular pattern is reticular, which is more organised in arrangement, and often approaches a plexiform. In some, primary reticular pattern is dominant, and only scattered Haversian systems are found. In other areas, often in the same bone, dense Haversian systems have entirely replaced the basic primary tissue.

In the bones of modern primates, the characteristic pattern is of longitudinal primary vascular structure. Primate bone tissue is distinctively lamellated, and the lamellae are deposited in a circumferential plane about the central marrow cavity. Much of the compact bone is densely vascularised, and some areas of the compact bone do not contain any vascularisation, while other regions showed a few, scattered canals. All primate bones are not necessarily composed of dense Haversian tissue, as there are some areas containing extensive primary vascular areas, while others have massive lamellation with scattered Haversian systems. Studies have also shown the presence of osteon banding pattern in a dog's bone (Ubelaker, 1999), and plexiform bone in young monkeys and human (Enlow, 1963). In brief, the descriptions of bone histologic patterns in various animals have provided useful information for identification purposes of animals.

Additionally, bone microstructural measurements were useful in the identification of human and nonhuman (Dix *et al*., 1991; Jowsey, 1966; Owsley *et al*., 1985; Pirok *et al*., 1966). Studies have produced measuring ranges for microstructural parameters such as osteon count (*OC*), osteon area (*OA*) and Haversian canal diameter (*HCD*) in human (Dix *et al*., 1991; Pirok *et al*., 1966) (Table 1), and osteon diameter (*OD*) and Haversian canal perimeter (*HCP*) in human and animals (Jowsey, 1966) (Table 2). There were fewer osteons and larger Haversian canals in human than in deer (Owsley *et al.*, 1985). In brief, microscopic method is useful to identify human and nonhuman skeletal remains.

Table 1 The microstructural parameters of human and deer bone thin sections by Owsley *et al.* (1985), Pirok *et al.* (1966) and Dix *et al.* (1991).

Parameter (mean)	Owsley *et al*., (1985)		Pirok *et al*., (1966)	Dix *et al*., (1991)
	Human (n = 1)	Deer (n = 1)	Human (n = 326)	Human (n = 1)
CT (*mm*)	3.75	3.3	-	-
OC (ct/mm^2)	1.06	5.92	16.6 ± 4.7	
HCD (μm)	177	71	60 ± 34	-
OA (μm^2)			0.03 - 0.05 ± 0.01	0.05 ± 0.01
OD (μm)			270 ± 35	-

Table 2 The microstructural parameters of human and animal bone thin sections by Jowsey (1966).

Animal	*n*	*OD* (μm)	*HCP* (μm)
Rat	3	72 ±14	36 ±12
Rabbit	6	98 ± 22	54 ± 24
Cat	6	163 ± 30	102 ± 36
Dog	4	154 ± 38	85 ± 37
Monkey	2	216 ±52	167 ± 46
Human	26	223 ± 50	173 ± 45
Cow	4	250 ± 40	213 ± 47

The table shows that the microstructural measurements were increasing in values from rat to the biggest animal, cow.

1.5 Age estimation in human bone based on the bone remodelling process

Age estimation in human bone has been based on the bone remodelling process, whereby the accumulation of osteons in adult life has been shown to have strong correlations with the age of an individual (Stout, 1998). Generally, bone resorption increased with age, and bone formation decreased with age, resulting in increased osteon fragments (Narasaki, 1990) and decreased *OC* (Ericksen, 1980), respectively.

Additionally, microstructural measurements in bone have been shown to vary among different populations and ethnic groups (Pollitzer and Anderson, 1989). For instance, the Nubian population have small Haversian canals due to increased bone formation

(Mulhern and Gerven, 1997), while the Southampton Island Eskimos have large Haversian canals and resorption spaces due to increased bone resorption (Thompson and Gunness-Hey, 1981). Between different ethnic groups, the European-American and African-American population differ in their microstructural measurements (Cho *et al*., 2002; Pratte and Pfeiffer, 1999). The European-American population have larger osteons than in the African-American population (Cho *et al*., 2002) (Table 3). Also, the European-American population has increased osteon count number compared to the African-American population (Pratte and Pfeiffer, 1999) (Table 3). Obviously, the study done by Cho *et al.* (2002) in both sample populations were taken from a higher age range that is, from 17 to 95 years of age for the African-American population and 17 to 82 years of age for the European-American population. This explains the increased *OC* number in both populations by Cho *et al.* (2002) compared to the Whites, Blacks and Colored by Pratte and Pfeiffer (1999).

Table 3 The microstructural parameters from different human populations by Pratte and Pfeiffer (1999) and Cho *et al.* (2002).

Microstructural parameter (mean ± *SD*)	Pratte and Pfeiffer (1999)			Cho *et al*. (2002)	
	Whites (n = 23)	Blacks (n = 20)	Colored (n = 19)	African-American (n = 103)	European-American (n = 51)
OC (*ct/mm*^{2})	15.71 ± 2.95	14.14 ± 3.26	14.93 ± 4.16	18.7 ± 0.71	20.07 ± 0.98
OA (*mm*^{2})	-	-	-	0.036 ± 0.001	0.039 ± 0.001

Age estimates based on the bone remodeling process in human vary between populations (Thompson, 1981), as shown by different microstructural values in different populations

(Pollitzer and Anderson, 1989). This has contributed to the production of regression equations specific for each population. For instance, age estimation in the *U.S.* Whites showed values comparable to the known ages by using the Whites regression equations. However, age estimation in the Eskimos showed some discrepancies in ages by using similar equations (Thompson, 1981). This has some impact on the calculation of age estimates in the population that it is necessary to have specific regression equations for each population (Aeillo and Molleson, 1993; Cho *et al*., 2002; Thompson and Gunness-Hey, 1981; Walker, 1990; Yoshino *et al*., 1994).

1.6 Aims and objectives of this study

Human and nonhuman identification and age estimation in skeletal remains may be achieved by doing histomorphometric analysis of human and nonhuman (mammal) bones. Literature showed that there were very few microstructural parameters studied in human and animal bones for identification purposes. Hence, the research question would be: 'What are the microstructural parameters that can be used for the identification of human and nonhuman skeletal remains? This study will study ten microstructural parameters in human and nonhuman bones for identification.

Literature has also shown that several microstructural parameters were used to produce age estimates in the European and American populations. Hence, the research question would be: 'What are the microstructural parameters that can be used to determine age estimation in human samples in the city of Kuala Lumpur, Malaysia? This study will study ten microstructural parameters for age estimation in human samples in Kuala Lumpur, Malaysia.

This study has two aims namely, to study ten microstructural parameters in human and animal bones for identification purposes, and to study ten microstructural parameters in human bones for age estimation. The objectives of this study were to produce discriminant functions for human and animal based on microstructural measurements for the identification of human and animal bone; and to produce produce age regression equations for human samples in Kuala Lumpur.

2. LITERATURE REVIEW

2.1 Identification of human and nonhuman bone

Identification of human and nonhuman in skeletal remains can be done by various methods such as microscopic, radiographic, immunologic and *DNA* or *RNA* analyses. The following sections will summarise the different methods of identification in human and animal with discussion of the main findings.

2.1.1 Microscopic method

Osteon banding is a distinct histologic feature, which can be found in midshafts of femoral bones in human and animals (Mulhern and Ubelaker, 2001). Osteon banding can be defined as a distinct row of five or more of primary and/or secondary osteons. There was a significant difference in osteon banding pattern between human and nonhuman bone ($P < 0.01$). The osteon bands are lined up in rows in nonhuman bone, whereas in human, the osteon bands were arranged randomly. The osteon bands were more abundant in nonhuman than in human, whereby 5 samples from 15 nonhuman samples showed osteon banding, and only 2 samples from 60 human samples showed osteon banding (Mulhern and Ubelaker, 2001). Further, the osteon bands were variable in lengths in nonhuman, whereas in human, there were uniform, shorter osteon bands. In conclusion, osteon banding is useful to differentiate between human and animal bone.

Plexiform bone, osteon banding, primary osteons and Haversian systems have also been examined in human and animal bones (Martiniaková *et al*., 2006), and the results revealed that the diaphysis of a human femur comprise entirely of dense Haversian system. Primary vascular plexiform was the basic histologic pattern in animals such as

pigs, cows and sheep. Additionally, numerous resorption cavities that are present between the Haversian systems were the main histologic feature in a pig's bone. Irregular Haversian systems in the periosteum and endosteum were found in a sheep's bone, while primary vascular longitudinal in the perioteum and endosteum was found in a rabbit's bone. Finally, a non-vascular tissue is a characteristic feature in a rat's bone. Additionally, microstructural measurements such *HCA*, *HCP*, *OA* and *OP* were found to be higher in human than in nonhuman. In brief, microstructural measurements and histologic pattern in bone are useful for human and nonhuman identification.

2.1.2 Radiographic method

The radiographic method has been used to identify human and nonhuman in skeletal remains (Chilvaquer *et al*., 1987). The radiographic features in human and animal long bones were found to be significantly different ($P < 0.001$). In human, the trabeculae in the midshaft area showed either circular or oblong trabeculae patterning, whereas in animal, the trabeculae showed a homogeneous granular appearance. Also, animal bone has a sharp border delineating the internal aspect of the cortex with small spicule-like invaginations and nutrient canals extending from the cortex to spongy bone in animal (Figure 11). However, some of the bones showed resemblance of both human and animal in their radiographic features resulting in difficulties to identify human and nonhuman (Chilvaquer *et al.*, 1987).

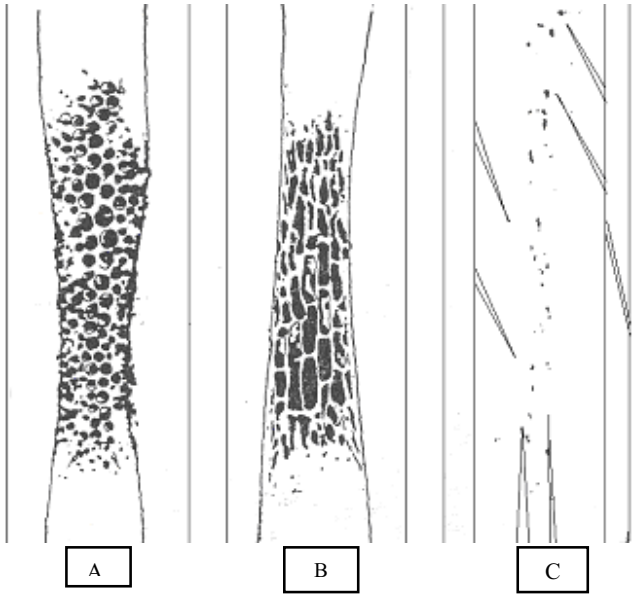

Figure 11 A diagrammatic representation of radiographic appearance of spongy human and nonhuman bone in midshaft of long bones (From Chilvaquer *et al.*, 1987).
Figure 'A' and 'B' shows human bones and 'C' shows animal bone (refer text).

Literature has shown that there were distinct radiological features in the tarsal and metatarsal bones in bear paws and human feet (Angel, 1974; Hoffman, 1984). Generally, the human foot tapers at the distal metatarsals, whereas bear paw has plantar ridges in the distal metatarsals (Angel, 1974; Hoffman, 1984; Owsley and Mann, 1990). Microstructural measurements in compact bones by microradiograph were also useful in the identification in human and swine (Imaizumi *et al*., 2002) (Table 4). In conclusion, radiographs of bone can be used in the identification of human and nonhuman.

Table 4 The microstructural measurements of human and swine by Imaizumi *et al.* (2002).

Specimen	*n*	*HCA(μm²)*	*HCD (μm)*
Human (radius)	35	4020 ± 2070	71.6 ± 19.8
Swine (scapula)	20	314 ± 181*	19.2 ± 5.6*

***P* < 0.001**
The table shows that Haversian canal size is smaller in swine than in human ($P < 0.001$).

2.1.3 Immunologic and chemical method

Protein radioimmunoassay is an immunologic method, which has been used to determine the identification of human and nonhuman skeletal remains (Ubelaker *et al*., 2004). The method involved extraction of albumin from the bone, followed by exposure to rabbit serum with species-specific antibodies, and to radioactively-labelled goat antibody. The measurement of radioactivity of the goat antibody was used to determine the most logical species represented. In certain circumstances, where there is little amount of amino acid or poor preservation of proteins, alterations in the protein content of bone will lead to false results.

Powder X-ray diffraction is a chenmical method, which has been used to examine bone mineral in human and animal for identification purposes (Beckett and Rogers, 2006). The method involved examination of the pyrolitic decomposition products and the rate of re-crystallisation of the bone mineral as determined by powder X-ray diffraction. Six species including human, cow, pig, sheep, turkey and rat were identified in a short period of time and at low cost. In conclusion, immunologic and chemical methods can also be used in the identification of human and nonhuman skeletal remains.

2.1.4 *DNA* and *RNA* analyses

New *DNA* technologies such as *STRs* typing and *mtDNA* have been utilised in forensic samples for human identification, whereby the nuclear *DNA* is either degraded or cannot be recovered in sufficient quantities (Butler and Levin, 1998; Cruz *et al*., 2004; Valente *et al*., 2004). The *STR* typing is successful only in cases, where a sufficient amount of *DNA* could be obtained, whereas *mtDNA* sequence analysis could positively identify

victims of crime cases or missing persons, where bodies remain undiscovered for many years (Bender *et al*., 2000).

Human *mtDNA* consists of a coding region, which contains the sequences for two ribosomal *RNAs*, 22 transfer *RNAs* and 13 proteins, and a noncoding region called the displacement loop (*D*-loop) or control region. By analysing regions within genomic, mitochondrial *DNA* (*mtDNA*) and ribosomal RNA (*rRNA*) as potential markers of differential *DNA* sequences, it is possible to detect genetic variants that aid in the discrimination of species. The forensic value of *mtDNA* arises from the sequence variability of the displacement loop (*D*-loop) between individuals, its efficient polymerase chain reaction (*PCR*) with limited biological material and its resistance to extreme environmental conditions. Further, thousands of copies of *mtDNA* may exist in a single cell, making it easier to recover and sequence than the single copy of nuclear *DNA* per cell. The controlled region of the *mtDNA* was estimated to vary about 1 to 3% that is, 1 to 3 nucleotides out of every 100 is different between unrelated individuals (Butler and Levin, 1998). Ribosomal ribonucleic acid gene is a locus found clustered on the *DNA* chromosome, which is known to possess regions of variation between species (Bellis *et al*., 2003).

The *mtDNA* and *rRNA* from blood specimen have been used in the identification of 10 human individuals and ten different animal species namely, domestic cat, chicken, cow, domestic dog, goat, horse, pig, rat, sheep and Bengal tiger (Bellis *et al*., 2003). It was found that human *DNA* can be distinguished from a limited number of animal species, and the most specific results were shown by the *TP53* gene, which could be used as a potential animal species identification tool.

The *rRNA* gene typing has also been used for identification of human and animals namely, Japanese monkey, dog, cattle, pig, cat, rabbit, mouse, rat, chicken, frog and fish (Naito *et al*., 1992). The band patterns obtained from each *DNA* sample differed in number and size, hence indicating the applicability of the method to species identification. Ribosomal ribonucleic acid typing can be done in minute degraded sample (1 *pg*). It can also be used for *DNA* of shorter length, which is often recovered from environmentally compromised samples.

Human skeletal remains from the Vietnam and other wars have been routinely analysed and identified by *mtDNA* for forensic identifications. Most of the forensic applications involve examination of *HV1* and *HV2* regions, where most of the variability between individuals is found. For instance, the *mtDNA* typing has allowed amplification of both hypervariable 1 (*HV1*) and hypervariable 2 (*HV2*) regions in *mtDNA* to determine the identification of human and swine in fragmented bones (Imaizumi *et al*., 2002). Imaizumi *et al.* (2002) have been able to examine fragmented bones, believed to have come from a woman, who was murdered and buried. Examination of the bones showed that the nucleotide sequence for *mtDNA* in the radius was identical to that of the victim's sister.

Also, *mtDNA* sequencing in the hypervariable 1 (*HV1*) and hypervariable 2 (*HV2*) control regions in *mtDNA* analysis has allowed maternal family relationships between three bodies in exhumed skeletal remains in Africa, where nucleotide substitutions were the same in two bodies and in a presumptive mother, suggesting a kinship relation (Cruz et al., 2004). The analysis of *mtDNA* was useful to determine maternal family relationships (Bender *et al*., 2000). Additionally, autosomal short tandem repeats (*STRs*) have also

been used to identify human, whereby positive results were obtained in 100% and 91% of cases in 25 femur and 22 vertebra human samples, respectively (Valente *et al*., 2004).

In *DNA* typing, *DNA* acid probes were developed to identify elk, deer and antelope (Blackett and Keim, 1992). The individual *DNA* sizes of different classes were used as hybridisation probes to identify antelope, elk and mule deer, and the hybridisation patterns for each probe is unique for each species. In this method, *DNA* was extracted from muscle cells to produce discrete bands of *DNA* by using electrophoresis gel, and only a minute amount of *DNA* of 1 μg is required for the method.

The repetitive *DNA* markers have been used for identification of white-tailed deer (*Odocoileus cirginianus*), moose (*Alces alces*) and black bear (*Ursus americanus*) (Guglich *et al*., 1994). A large amount of *DNA* (about 5 to 10 µg) is required for this method to reveal unique banding patterns for different species. The technique was found to be faster (less than 8 hours) and less expensive, compared to *DNA* acid probes, which was more time consuming (a few days) and more costly (Blackett and Keim, 1992). In conclusion, all of the above methods were useful in the identification of human and different animal species. Because of the fact that each method has some limitations, the microscopic method is considered the best method to be used in the identification of human and nonhuman skeletal remains.

2.2 Estimation of age at death in human bone based on remodelling process

2.2.1 Histologic method

2.2.1.1 Effects of ageing in bone microstructure

Microstructural measurements have been shown to be significantly correlated with age ($P < 0.001$) except for resorption spaces (Ericksen, 1991). Primary canals and lamellar bone were negatively correlated with age (Ericksen, 1991; Samson and Branigan, 1987), while all the other microstructural parameters namely, osteon count (Ericksen, 1991; Lynnerup *et al*., 2006), type II osteon count, osteon fragment count, primary osteon count, percent lamellae bone, percent osteonal bone and percent fragmented bone were positively correlated with age. Type II osteons (section 2.2.1.3) showed a tendency to increase with age, but resorption spaces remained constant. Primary osteon and percent of circumferential lamellae bone were found to decrease after the 4^{th} decade. In males, osteons increased in number steadily with each decade, while female osteon number reached a plateau in the sixth decade and then, remained constant. In both males and females, the osteon fragment count increased with age, but the increase is greater in females than in males. In females, osteon fragment count increased by the fifth decade in female, unlike in males, the osteon fragment count increased by the seventh decade.

Significant correlations were found between percent lamellar bone, osteon number, osteon fragment and primary osteon number and age ($P < 0.05$) (Kerley, 1965). Of the parameters, percent lamellar bone and primary osteon showed negative correlations with age. The remaining parameters showed positive correlations with age. Samson and Branigan (1987) found that osteon diameter had a positive correlation with age ($P < 0.01$).

The effects of ageing have been studied on the middle third of the 5th to 7th rib bone microstructure in 326 people, aged from birth to 98 years old (Pirok *et al*., 1966). The results showed that as people aged, there were increased *OC* with decreased *OD* and increased *HCD* resulting in numerous smaller osteons due to increased formation, but larger Haversian canals due to increased bone resorption, as remodelling activity increased after the age of 30 years old (Pirok *et al*., 1966). The *OA* increased with age and *HCA* either remained the same or increased with age. No significant trend was noted in *OC* per unit area (Black *et al*., 1974). In conclusion, microstructural measurements were useful for age estimation in human bone.

2.2.1.2 Age estimation in different human population

Histological analysis of the femoral bone showed that Eskimos contain more osteons per unit area than *U.S.* Whites (Thompson and Gunness-Hey, 1981). Differences were significant between 189 Eskimos and 144 Whites for osteon area ($P < 0.05$). These differences were caused by differences in osteon remodelling patterns between Eskimos and Whites. Results have shown that Eskimos femora tend to be thinner than those of *U.S.* Whites due to faster rates of age-related bone loss in living Eskimos. According to the study, the adult Eskimos lived in St. Lawrence Island, North Alaska and Canada, while the *U.S.* Whites lived in the United States. As both sample populations lived in different places and have different lifestyle, environment and diet, these factors could have contributed to the difference in osteon remodelling patterns between the Eskimos and Whites.

In the estimation of ages in Eskimos skeletons by using regression equations generated in *U.S.* Whites, it showed ages exceeding those obtained by morphologic methods such as

cortical thickness, bone mineral content and cortical bone density. This was true for Eskimos morphologically aged less than 35 years, where morphologic ages were found to be more accurate. Age estimates in Whites by using regression equations generated in *U.S.* Whites were found to be aged accurately.

Literature also showed that the Eskimos from Baffin Island in a sample of 44 skeletons have thin femoral cortices and increased *OC* than in the *U.S.* Whites. The findings of increased *OC* were applicable to other Eskimo groups from Southampton Island, Greenland, St. Lawrence Island and Kodiak Island (Thompson and Gunness-Hey, 1981). The implications of increased *OC* in the Eskimos implied that the rates of bone remodelling were slightly higher in Eskimos than in the *U.S.* Whites. Age estimates using equations generated for U.S. Whites tend to overage Eskimo skeletons. Age estimates as determined by morphologic and histologic methods showed good estimates in individuals aged more than 35 years of age, but poor estimates in individuals less than 35 years of age (Thompson *et al*., 1981). This finding supported the necessity of population-specific age regression equations for Eskimo population.

Continuous remodelling of bone in response to the metabolic and biochemical needs of the body results in higher *OC* in cortical bone with increasing age. The type of physical activity in an individual can also influence bone microstructure, as biomechanical factors influence amount and location of remodelling activity (Frost, 1973) leading to distinctive bone microstructure in a human sample population. In conclusion, each population has shown different values of microstructural measurements, which requires a specific age regression equation for each population to provide accurate age estimates for the population.

2.2.1.3 Definitions in bone microstructure

Definitions of microstructural parameters were found to vary in previous studies. For instance, osteon population density is used to represent both osteon and osteon fragment (Pratte and Pfeiffer, 1999; Stout and Paine, 1992). Intact osteon density was defined as the number of Haversian system with at least 90% of the perimeter of Haversian canal present divided by the cortical area. The fragmentary osteon density was defined as the number of remodelled Haversian systems including those with at least 10% of their Haversian canal present divided by the cortical area. These definitions were used in age estimation studies in rib cortical bones (Pratte and Pfeiffer, 1999).

In a study by Ericksen (1991), the definitions for Haversian system and osteon fragments were slightly different from previous studies. A Haversian system is an osteon with an intact Haversian canal, and not breached by a resorption space or impinged by the walls of a later osteon. A type II osteon has two concentric cement lines. It formed from resorption in the Haversian canal of a Haversian system. The new resorption space is small and has a cement line, filled in with new lamellae forming an osteon-within-an-osteon structure. The inner cement line does not touch the outer one at any point.

Osteon fragments were defined as remnants of former osteons, which ranged from tiny slivers to full-sized 'dead' osteons with Haversian canals showing Howship's lacunae. Resorption spaces are spaces with scalloped edges formed by Howship's lacunae, which range from breakthrough of the wall by a vessel in lamellar bone or within a Haversian canal of an osteon to the large resorption cavities in the bones. In conclusion, definitions for microstructural parameters have to be established before measurements can be taken for age estimation in a sample population.

2.2.1.4 Observational error analysis

Observation tests in histomorphometric studies have shown that observers were found to be more confident in viewing histologic structures when they have many years of experience in the field. Both experienced and inexperienced observers were found to have problems identifying bone microstructures hence, accounting for the large variability among observers (Lynnerup et al., 1998). The intra-observer analysis showed significant variations in Haversian canal count ($P < 0.05$), whereas inter-observer analysis showed variation in osteon fragment count and Haversian canal count ($P < 0.05$). Additionally, observer comparability showed the largest standard error in the histological method, in which the identification of osteons was more vulnerable to the experience of the observer (Baccino *et al*., 1999).

Haversian canals were variable in structures causing difficulties in differentiating between a Haversian system and a primary canal (Lynnerup *et al*., 1998). Haversian canal can be identified easily as it has delimitation by a cement line, unlike primary canals, which do not have a cement line. However, observers may not be able to identify the cement line, even under high magnification. Many studies have done osteon counting to represent both Haversian system and osteon fragment, as differentiation of both structures may prove difficult (Cho *et al*., 2002; Frost, 1987a; Frost, 1987b). Lynnerup et al. (1998) have shown that using osteon fragment count in age regression would cause an error in age estimates. By excluding osteon fragment count from regression formulas, it would limit the use of the method to adults in the age range of 20 to 40, as osteon fragment predominates in older individuals. Hence, the use of *OC* to include both Haversian

system and osteon fragment would be useful. In conclusion, observation of osteon as the most identifiable structure, has been used by researchers for age estimation.

2.2.2 Other age estimation methods

Examination of single-rooted teeth, sternal end of the fourth rib, symphyseal face of the pubis, and femoral cortical remodeling have been used for age estimation in 19 adult individuals (Baccino *et al*., 1999). The percentage of circumferential lamellar bone, primary osteon count, osteon count and osteon fragment count at the periosteal border of the cortex were analysed to study the femoral cortical remodelling. Baccino et al. (1999) showed that combined methods were superior to individual ones, as they have potential for greater accuracy than either alone.

A histomorphologic method was used to perform age estimation in cremated remains from two urn fields in Germany (Cuijpers and Schutkowski, 1993). The morphologic criteria used were teeth eruption, fusion of epiphyses and closure of cranial sutures, while histologic criteria were qualitative and quantitative study of bone microstructures. The qualitative study measured the internal and external circumferential lamellae thickness, and analysis of the number and arrangement of osteon and resorption spaces with advancing age, while the quantitative study included *OC*. Results showed that both qualitative and quantitative study of bone microstructures were useful for age estimation in adult individuals (Cuijpers and Schutkowski, 1993).

A combination of a macroscopic method and microscopic method has been used to assess age estimation in 387 individuals from the crypt of Spitalfields, London from stillborn to 92 years old (Aeillo and Molleson, 1993). Aeillo and Molleson (1993) studied the macroscopic method, the Acsádi and Nemeskéri (*AN*) pubic ageing method, which

involved examination of pubic symphysis in relation to age. The two microscopic methods, the Kerley and Ubelaker's (1978) and the Samson and Branigan's (1987) methods involved microstructural measurements in the outer cortex and deeper cortex of midshaft of femoral cortex, respectively. Results showed that the percentage lamellar bone was a reliable parameter to differentiate between younger and older individuals, and those above 45 year age group had consistently showed 20% or less lamellar bone. Further, the most accurate age estimates especially in the 20 to 40 year age group was to combine histological ageing with pubic symphysis ageing (Aeillo and Molleson, 1993). Additionally, Suchey-Brooks method for pubic symphysis, Lovejoy method for auricular surface, Lamendin method for monoradicular teeth and Işcan method for fourth rib were used in age estimation in 98 White samples and 120 Black samples, with the ages ranged from 25 to 90 years from the Terry collection in the Smithsonian Institution's National Museum of Washington (Martrille *et al*., 2007). In conclusion, combination of methods is useful in age estimation in human population.

2.3 Other uses of bone microstructure in human

Microstructural measurements have been used to determine sexual dimorphism in bone (Dupras and Pfeiffer, 1996). Dupras and Pfeiffer (1996) analysed cortical area, osteon area and Haversian canal area in the ribs of 244 adults from the crypt of Christ Church in Spitalfields, East London. They found that female ribs were smaller that is, approximately 75% the size of male ribs. Male and female samples were shown to be significantly different in their microstructural measurements ($P < 0.001$). The mid-thoracic rib cross section has been reported to show greater sexual dimorphism than at other locations on the ribs. Discriminant function analysis showed that males may be

differentiated from females in 85% of cases. However, the correct classification rate is higher when using only morphologic parameters with 88% of success rate. Hence, morphologic parameters of the ribs are better sex predictors than histologic parameters.

3. MATERIALS AND METHOD

3.1 Bone materials

A sample of 64 adult human long bones was collected from the mortuary of Universiti Kebangsaan Malaysia Medical Centre (*UKMMC*), Kuala Lumpur, Malaysia, while 65 non-human (mammal) long bones were collected from the Zoos of Taiping and Kuala Lumpur. The bones were collected from human subjects, who were not known to have any bone diseases from previous medical records. From 64 human individuals, 9 of them had diabetes mellitus; however the bones were healthy and showed no signs of bone diseases. The human samples comprised 50 male and 14 female samples. The human samples were not homogeneously sampled due to religious inhibitions and the availability of cases, which reflected on the daily practice of forensic pathology in the medical centre, the main forensic centre in Malaysia. The human samples were mainly victims of road traffic accidents. The male samples were within the age range of 21 to 78 years (mean = 41.68 years), while the female samples were within the age range of 22 to 91 years (mean = 43 years). The procedure for legal handling of human bones was stated in the Criminal Procedure Code Section 331 (*CPC* Section 331) that it is mainly for investigation purposes (Figure 21 - Appendix 5). A medical document was obtained from the medical centre, which stated that the bones were transported for research purposes (Figure 22 – Appendix 5).

Figure 12 Map of Malaysia
The arrow shows Kuala Lumpur city, where human and animal samples were collected. It is located in the peninsula of West Malaysia (Anonymous, 2009)

The human population in Malaysia (Figure 12) comprised three major and four minor races. The major races comprise the Malays, Chinese (from Southern China) and Indians (from Southern India) were Malaysian citizens, while the minor ones were immigrants from Indonesia, Pakistan, Bangladesh and Myanmar. In this study, human bones were collected from races namely, Chinese (n = 43), Indian (n = 13), Indonesian (n = 3), Malay (n = 2), Myanmar (n = 1), Pakistani (n = 1) and Bangladeshi (n = 1) (Appendix 1). Different types of human bones were collected namely, humerus (n = 26), radius (n = 19), tibia (n = 7), femur (n = 9), fibula (n = 2) and ulna (n = 1).

The animal bones comprised 26 different animal species namely, black panthers (*Panthera pardus*, *n = 5*), cows (*Bos indicus, n = 9*), deer (*Cervus spp. , n = 6*), banded-leaf monkeys (*Presbytis femoralis, n = 2*), sheep (*Ovis arie, n = 5*), sambar deer (*Cervus*

unicolo, n = 1), Rhesus macaque (*Macaca mulatta, n = 1*), goats (*Capra hircus, n = 3*), Malay civet (*Viverra tangalunga, n = 2*), Bawean deer (*Cervus kuhlii, n = 1*), pig-tailed macaque (*Macaca nemestrina, n = 4*), bearcats (*Arctictis binturong, n = 2*), greater mousedeer (*Tragulus napu, n = 2*), buffalo (*Bubalus bubalis, n = 1*), leopard cats (*Prionailurus bengalensi, n = 6*), serows (*Capricornis sumatrensis, n = 2*), slow loris (*Nycticebus coucang, n = 1*), flat-headed cat (*Prionailurus planiceps, n = 1*), large Indian civet (*Viverra zibetha, n = 3*), common palm civet (*Paradoxurus hermaphroditus, n = 2*), pygmy hippopotamus (*Cheoropsis liberiensis, n = 1*), silver-leaf monkey (*Trachypithecus cristatus, n = 1*), long-tailed macaque (*Macaca fascicularis, n = 1*), mousedeer (*Tragulus javanicus, n = 1*), white-handed gibbon (*Hylobates lar, n = 1*), and rabbit (*Oryctolagus cuniculus, n = 1*) (Appendix 2).

The animal samples (mammals) were not homogeneously collected, as the sample were collected depending on the availability of cases in the Zoos, whereby the animals were either dead due to predator attack or died of old age. The animal bones comprised humerus (*n = 5*), radius (*n = 15*), tibia (*n = 9*) and femur (*n = 36*). The fact that there was limited access to the number of animal species and their bones, as well as, the number of human bones and their bones, this has contributed to some restrictions in the final analysis as the results obtained were not fully representing the general population.

A medical document was obtained from the medical centre, which stated that the bones were transported for research purposes (Figure 22– Appendix 5). A permit for the bones was obtained from the 'Ministry of Wild Life of Malaysia', which authorised the export of bone overseas for research purposes (Figure 23 – Appendix 5).

3.2 Method

3.2.1 Preparation of bone thin section

The method used in this study to produce bone thin sections was based on a standard bone preparation. The bone was cut from the mid-shaft of long bones at 3 cm lengths. Cortical thickness and medullary cavity diameter were measured by using digital calipers (Absolute Digimatic, Japan) (Appendix 4). The bone was de-fatted in diethyl ether solution (Fischer Scientific Int. Co., *UK*) (Appendix 4) for 24 hours in a sohxlet-condenser, which consists of a glass flask, an extraction chamber, and a distillation chamber.

The bone was embedded in a mixture of epoxy resin (Buehler, Dusseldorf) (Appendix 4), which was prepared by adding 100 parts of epoxy resin (Buehler Epo-thin low viscosity) to 36 parts of hardener (Buehler Epo-thin Epoxy hardener). The bone was placed in a vacuum chamber for half hour to remove any air bubbles in the resin, and facilitate resin penetration into the bone. Sectioning of bone was done by using the microtome (*LEICA SP* 1600, Germany) (Appendix 4) to produce a face cut. A glass slide was glued to the bone face cut, and cured with ultra violet light for 30 seconds before sectioning at 30 microns was done.

3.2.2 Examination of bone thin section

The bone thin section was examined under a transmitted light microscope (Olympus *BX51M*, Japan) (Appendix 4) at 100x magnification, and the images were captured by using a camera (Olympus *DP* 70, Japan) (Appendix 4), which is mounted on the microscope. The images were transmitted to the '*SIS* Soft Imaging System' image

analyser, where the image was calibrated by using an objective micrometre (*AX0001*, Olympus, Japan) (Appendix 4). A square grid of 10x10 microns (Figure 14) was superimposed on four subperiosteal locations that is, antero-medial, antero-lateral, postero-medial and postero-lateral on the bone thin section for microstructural measurements (Figure 13). The bone cross section was divided into four equal quadrants, and each quadrant was divided into two halves so that two locations were placed on each side of the line, separated by a square grid of 100 microns^2. The posterior aspect of the cross section was excluded to avoid the linea aspera, where most of the histologic variation occurs.

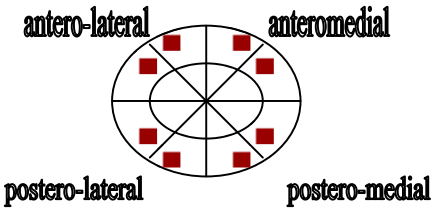

Figure 13 The bone cross-section indicating the fields for microstructural measurements.
The figure shows four different quadrants for microstructural measurements namely, anteromedial, anterolateral, posteromedial and posterolateral. Each quadrant is divided into one half to produce two sub-fields, one on each side of the line, so that eight fields were measured in total.

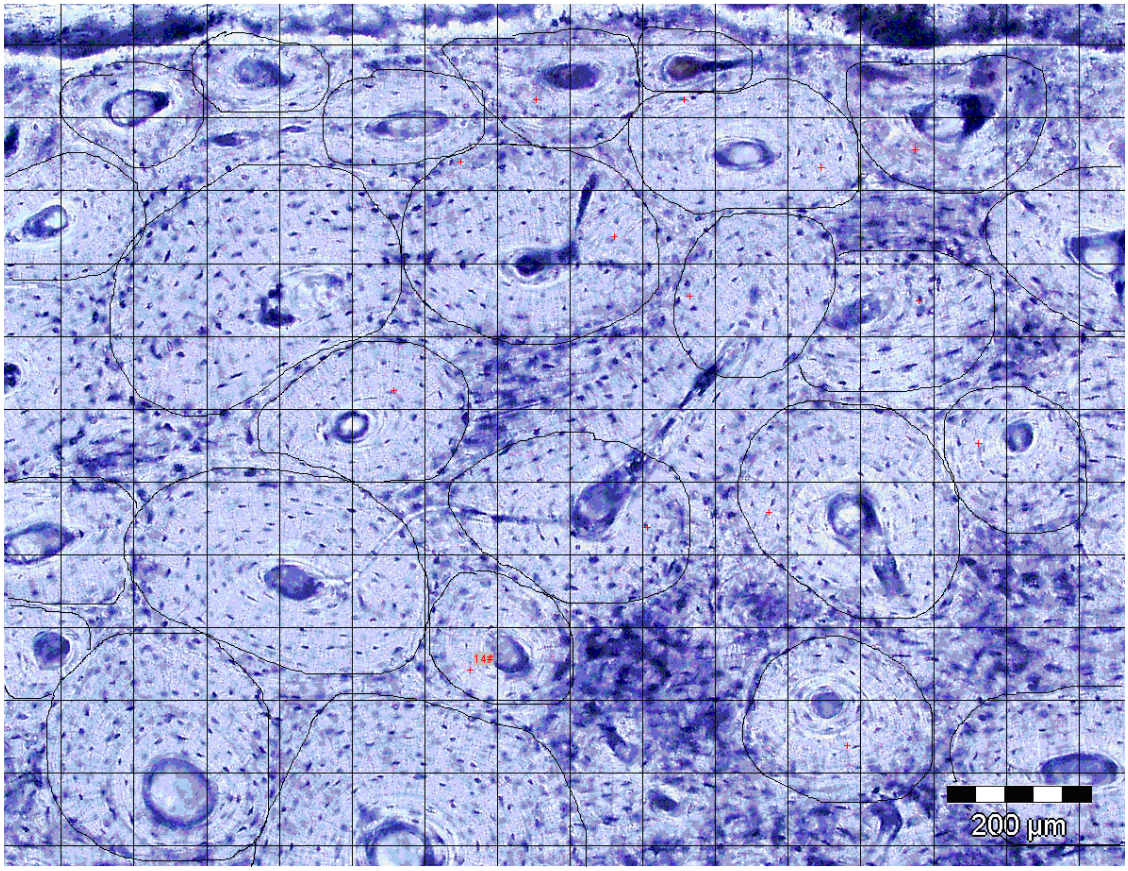

Figure 14 The photomicrograph of a human radius thin section (This study).
The grid 10x10 μm (100 μm^2) was superimposed on the subperiosteal location on the bone thin section. The Haversian systems are shown as marked structures.

In this study, assessments were made on ten microstructural parameters namely, cortical thickness (*CT*), medullary cavity diameter (*MCD*), osteon count (*OC*), osteon diameter (*OD*), osteon area (*OA*), osteon perimeter (*OP*), Haversian canal diameter (*HCD*), Haversian canal area (*HCA*), Haversian canal perimeter (*HCP*), and Haversian lamellae count (*HLC*) within a square grid of 100 micron^2, and the measurements were made by using the image analyser.

In this study, microstructural parameters were defined by using the definitions described by Ericksen (1991). Haversian system (Figure 14) is defined as an osteon with its

Haversian canal intact, and not breached by a resorption space or impinged upon by later osteon, while osteon fragment (Figure 15) is defined as remnants of Haversian system which may range from tiny slivers to full-sized osteons with Haversian canal showing Howship's lacunae (Ericksen, 1991).

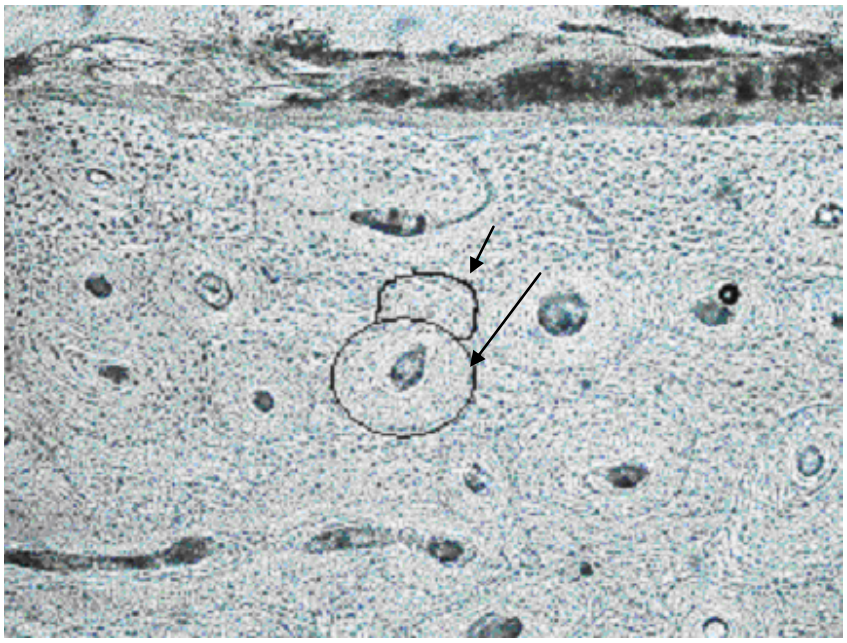

Figure 15 The photomicrograph of a human radius thin section (100x magnification).
The long arrow indicates a Haversian system, while the short arrow indicates an osteon fragment.

The counting of osteon was done by using a mouse click on the structure. The *OA* and *OP* (Figure 16) were measured by marking the boundary of an osteon by mouse clicking. Similarly, *HCA* and *HCP* were measured by marking the boundary of the Haversian canal. The *OD* (Figure 17) was measured by taking the mean of the maximum and minimum *OD* across the osteon, drawn perpendicular to each other. The diameter of Haversian canal was measured by taking the mean of the maximum and minimum *HCD* across the Haversian canal, drawn perpendicular to each other. The *HLC* was done by

using a mouse click on each lamella of the osteon, and taking the mean of *HLC* on two perpendicular sides of the osteon (Figure 18). The *CT* of bone was measured by taking the mean of the maximum and minimum *CT* of the bone by using the digital calipers. The *MCD* was measured by taking the mean of the maximum and minimum diameters of *MCD* by using the digital calipers.

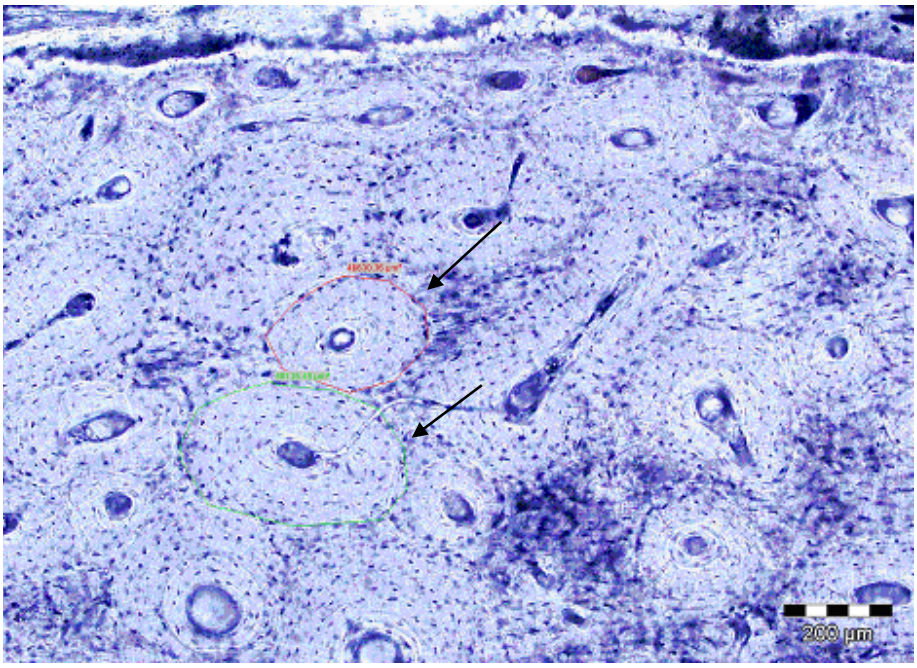

Figure 16 The photomicrograph of a human radius thin section (This study).
The *OA* and *OP* were measured by marking the boundary around each osteon (shown by arrows).

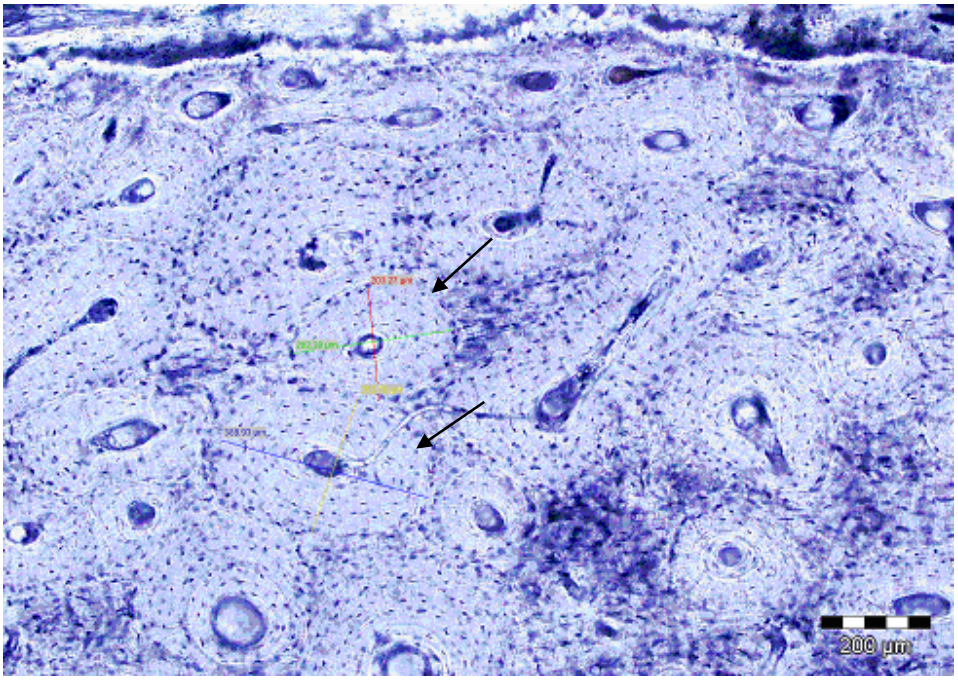

Figure 17 The photomicrograph of a human radius thin section (This study).
The *OD* was obtained by taking the mean of two perpendicular lines drawn across the Haversian system to indicate the minimum and maximum diameters (shown by arrows).

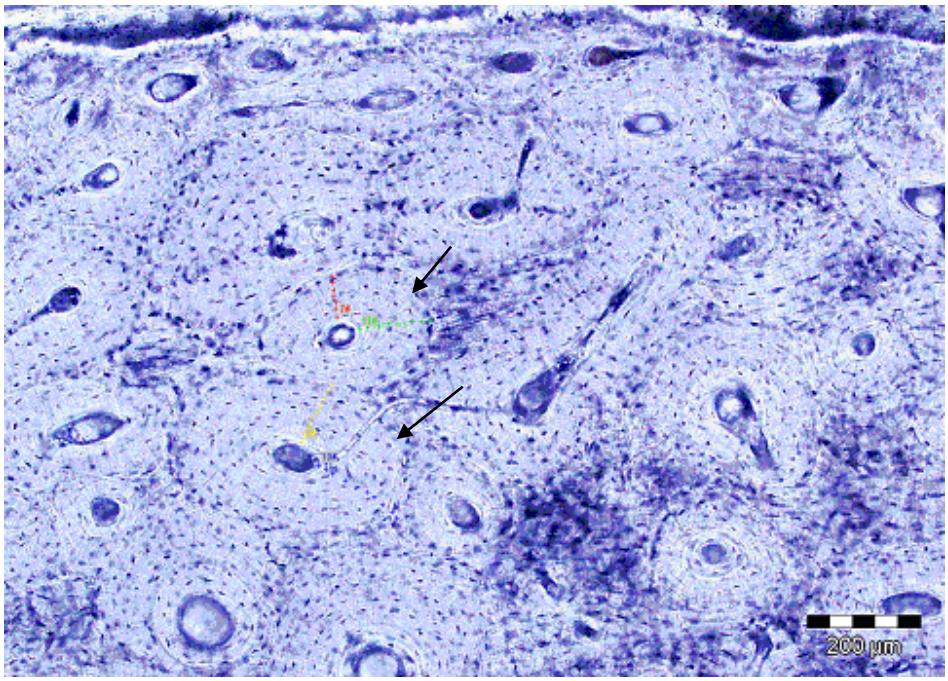

Figure 18 The photomicrograph of a human radius thin section (This study).
The *HLC* was obtained by taking the mean of *HLC* on two perpendicular sides of the Haversian system (shown by arrows).

3.2.3 Inclusion and exclusion criteria

In this study, the criteria was modified from that previously described by Wachter *et al.* (2002) in that the osteon count was counted as to include both osteon and osteon fragment. The osteon with half and /or more than half of its *HC* present within the field was counted. An osteon fragment at the periphery of the field was also counted, although it was present only partly within the field (Wachter *et al*., 2002).

Measurement of osteon was done according to the following criteria. Firstly, the osteon border must be fully intact. Next, the Haversian canal (*HC*) must be fully intact, but *HC* that merges with Volkmann's canal was excluded from measurement. Finally, an osteon at the periphery of the field was measured, if all of the above criteria were fulfilled. The exclusion criteria were applied in animal bone, where any area exhibiting plexiform bone pattern was excluded from measurements, as the area devoid of secondary osteons.

3.2.4 Observational error analysis

In this study, three independent observers were involved in the observational analysis. The first observer is a forensic anthropologist with vast experience in the field, the second observer is a forensic archaeologist also with vast experience in the field, and the third observer is a forensic pathologist (the author) with a few years experience in the field.

Definitions of the microstructural parameters were given beforehand to the observers, and they were given a short session to identify the histologic structures. Ten human bone thin sections were evaluated by each observer under 100x magnifications. They were required to do *OC* in the anteromedial field on each slide, within 100 micron^2 field by using a

transmitted light microscope and an image analyser. The *OC* was done without any knowledge of the sample's age, origin or type of bone for blinding purposes. The second analysis of *OC* was repeated after one week interval.

3.2.5 Statistical methods

In this study, a statistical package (SPSS for windows, Version 13.0) was used to analyse the results. The sample size for human and animal samples were sufficient by using the statistical power calculations (Bland, 1995). Ten bone microstructural parameters were measured as dependent variables in human and animal samples. The Kolmogorov-Smirnov (*K-S*) test for microstructural measurements in human and animals showed an abnormal distribution. Hence, the Mann-Whitney *U*-test was used to compare the microstructural measurements between human and nonhuman. The 'case diagnostic test for residual (outliers)' did not detect any residuals in the samples. Stepwise discriminant function analysis was used to produce discriminant functions for human and nonhuman by using various combinations of the 10 microstructural parameters.

Ten microstructural parameters were measured as dependent variables in human male and female samples, and they showed a normal distribution by using the Kolmogorov-Smirnov (*K-S*) test. The independent sample *t*-test of the microstructural measurements did not show any significant difference between male and female samples. The Pearson's correlation test was used to determine the correlations between microstructural measurements in human and age. The 'case diagnostic test for residuals' showed the presence of two residuals, which were removed from the regression analysis. The multivariate regression analysis was used to produce age regression equations in the human samples. Paired *t*-test was used to analyse the difference in *OC* between the first

day and the seventh day in each observer. One-way analysis of variance (*ANOVA*) was used to analyse the difference in *OC* between the three observers.

4. RESULTS

4.1 Human and nonhuman bone microstructure

There were 64 human bones were collected from the mortuary of Universiti Kebangsaan Malaysia Medical Centre (*UKMMC*), Kuala Lumpur, and 65 animal bones collected from the Zoos in Taiping and Kuala Lumpur. Two slides of bone thin sections were prepared from each sample for the analysis of microstructural measurements, and their values were taken and averaged (Table 5). The null hypothesis in this study was to show that there was no difference in microstructural measurements between human and nonhuman (mammal) bone. As both human and nonhuman samples showed skewed distributions, the Mann-Whitney test was used to test the difference between the two sample populations. By using the Mann-Whitney test, the microstructural measurements showed significant differences between human and non-human bone ($P < 0.001$) (Table 6). The box-and whiskers plot also showed that *OC* in human (mean = 14.57; *SEM* = 0.54; n = 64) was higher than in animal (mean = 7.45; *SEM* = 0.86; n = 65) (Figure 19). The fact that the human and animal species and their types of bones were sampled heterogeneously, the microstructural differences have to be taken with caution.

Table 5 Descriptive statistics of microstructural parameters for human and animal bone thin sections.

	Human/animal	*N*	*Mean ± SEM*
OC ($ct/\mu m^2$)	Human	64	14.57 ± 0.54
	Animal	65	7.45 ± 0.86
HCD (μm)	Human	64	50.05 ± 0.92
	Animal	65	32.48 ± 3.16
HCA (μm^2)	Human	64	1953.49 ± 7.89
	Animal	65	1475.93 ± 26.63

HCP (μm)	Human	64	177.28 ± 3.22
	Animal	65	119.00 ± 11.05
HLC (*ct*/osteon)	Human	64	3.43 ± 0.24
	Animal	65	2.70 ± 0.22
CT (*mm*)	Human	64	4.90 ± 0.16
	Animal	65	3.35 ± 0.25
MCD (*mm*)	Human	64	10.04 ± 0.37
	Animal	65	8.37 ± 0.68
OD (μm)	Human	64	199.62 ± 2.31
	Animal	65	132.74 ± 8.59
OA (μm^2)	Human	64	33285.55 ± 8.69
	Animal	65	17781.8 ± 14.09
OP (μm)	Human	64	702.4 ± 9.09
	Animal	65	456.06 ± 29.50

The table shows that the microstructural measurements were greater in human than in nonhuman.

Table 6 Mann-Whitney test of microstructural parameters for human and animal bone thin sections.

	OC	*HCD*	*HCA*	*HCP*	*HLC*	*CT*	*MCD*	*OD*	*OA*	*OP*
Mann-Whitney	765.00	625.00	771.00	711.00	1513.50	946.00	1414.50	412.000	416.00	378.00
Wilcoxon	2910.00	2770.00	2916.00	2856.00	3658.50	3091.00	3559.50	2557.000	2561.00	2523.00
Z	-6.19	-6.85	-6.16	-6.45	-2.67	-5.34	-3.13	-7.860	-7.84	-8.02
Sig. (2-tailed)	.001**	.001**	.001**	.001**	.008**	.001**	.002**	.001**	.001**	.001**

a Grouping Variable: human/animal
**** ($P < 0.001$)**

The table shows that the microstructural measurements were significantly different between human and animal.

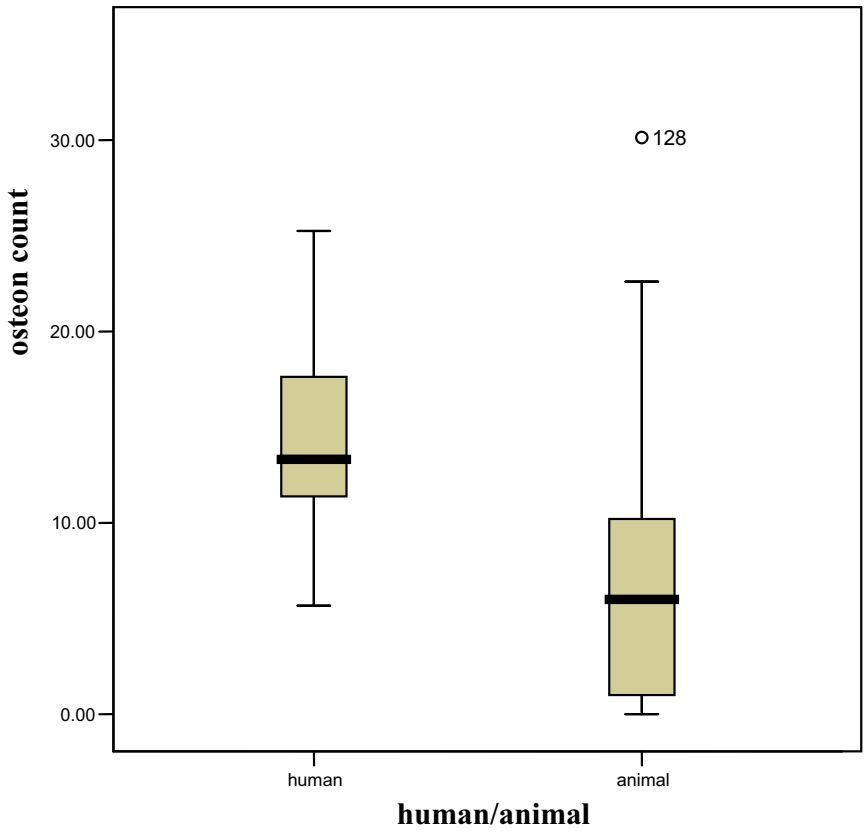

Figure 19 Box-and whisker plots of *OC* for human and animal bone thin sections. In the plots, the horizontal line in the centre of the box represented the median value of *OC*. The inter-quartile range of *OC* was indicated by the box, while the range of *OC* from maximum to minimum quartiles was shown by the whiskers at the end of each box. An animal sample that is, *Paradoxus hermaphroditus* (common palm civet) was lying outside the box and whiskers, but it was still within the normal range.

Figure 19 showed that there is an overlap in the data distribution between human and nonhuman, and this may be attributed to the heterogeneous sampling of both human and nonhuman samples, as well as, the heterogeneous sampling of the types of bones for each individual human and nonhuman species. The heterogeneous sampling was obviously due to restricted time of sampling, which has limited the research study to work on limited number of human and nonhuman species and their types of bones.

Since the microstructural measurements for both human and nonhuman bones showed a skewed distribution, some of the data was converted to logarithmic values to normalise the data distribution. The microstructural parameters were analysed by using discriminant function analysis to produce discriminant functions for human and animal. The analysis was based on six microstructural parameters ($P < 0.001$; Wilk's $\lambda = 0.359$; $\chi^2 = 114.884$; $df = 6$) (Table 7), allowing a canonical discriminant function (D) to be employed (Table 8):

$$D = -40.942 + 3.007\,(log\ HCA) + 2.867\,(log\ HLC) + 11.749\,(log\ OP) + 0.097\,(OC) + 0.069\,(HCD) - 0.029\,(HCP)$$

Table 7 Summary of canonical discriminant functions.

Test of Function(s)	Wilks' Lambda	Chi-square	*df*	*Sig.*
1	.359	114.884	6	.001

The table shows that the discriminant function was based on 6 microstructural parameters at $P < 0.001$.

Table 8 Unstandardised canonical discriminant function coefficients.

	Function 1
log_HCA	3.007
log_HLC	2.867
log_OP	11.749
OC	.097
HCD	.069
HCP	-.029
(Constant)	-40.942

The table shows the discriminant functions for each parameter, which form the discriminant function equation.

The discriminant functions showed correct classification rates for 81.4% of cases, with identification accuracy of 96.9% for human and 66.2% for animal ($P < 0.001$). A positive value indicated human, while a negative value indicated animal (Table 9). On cross

validation, the discriminant functions showed correct classification rates for 79.1% of cases, with identification accuracy of 95.3% for human and 63.1% for animal (Table 10).

Table 9 Unstandardised canonical discriminant functions evaluated at group means.

	Function
	1
Human	1.207
Animal	-1.457

The table shows that a positive discriminant function indicates human and a negative function indicates nonhuman.

Table 10 Classification rates for human and animal bones.

			Predicted Group Membership		Total
			Human	Animal	
Original	Count	Human	62	2	64
		Animal	22	43	65
	%	Human	96.9	3.1	100.0
		Animal	33.8	66.2	100.0
Cross-validated	Count	Human	61	3	64
		Animal	24	41	65
	%	Human	95.3	4.7	100.0
		Animal	36.9	63.1	100.0

The table shows high classification rates for human and nonhuman in original and cross-validated groups.

4.2 Human male and female bone microstructure

The microstructural measurements in male and female samples showed a normal data distribution by using the *K-S* test (Table 11). The descriptive statistics of microstructural measurements (Table 12) showed female has thinner cortical bone with fewer osteons, larger osteons and larger Haversian canals than in male. However, the independent sample *t*-test of the microstructural measurements did not show any significant difference between male and female samples (Table 13).

Table 11 Kolmogorov-Smirnov test of microstructural parameters for human male and female bone thin sections.

sex		*OC*	*HCD*	*HCA*	*HCP*	*HLC*	*CT*	*MCD*	*OD*	*OA*	*OP*
male	*N*	50	50	50	50	50	50	50	50	50	50
	KS	1.03	0.95	1.14	1.14	1.01	0.87	1.06	0.76	0.79	0.73
	Sig. (2-tailed)	0.23	0.32	0.14	0.14	0.25	0.42	0.21	0.59	0.54	0.66
female	*N*	14	14	14	14	14	14	14	14	14	14
	KS	0.46	0.53	0.66	0.58	0.72	0.50	0.86	0.61	0.83	0.60
	Sig. (2-tailed)	0.98	0.93	0.76	0.88	0.66	0.96	0.44	0.84	0.49	0.86

The table shows a normal data distribution (significance level more than 0.05).

Table 12 Descriptive statistics of microstructural parameters in male and female bone thin sections.

		N	Mean	*SEM*
OC (ct/μm^2)	Male	50	14.74	0.60
	Female	14	13.98	1.3
HCD (*μm*)	Male	50	49.57	1.01
	Female	14	51.73	2.25
HCA (*μm*^{2})	Male	50	194.28	9.48
	Female	14	199.80	12.97
HCP (*μm*)	Male	50	177.20	3.72
	Female	14	177.56	6.56
HLC (*ct*/osteon)	Male	50	5.90	0.28
	Female	14	5.97	0.49
CT (*mm*)	Male	50	5.00	0.18
	Female	14	4.53	0.38
MCD (*mm*)	Male	50	10.1	0.40
	Female	14	9.86	0.95
OD (*μm*)	Male	50	198.34	2.69
	Female	14	204.20	4.41
OA (*μm*^{2})	Male	50	327.77	10.3
	Female	14	351.05	14.66
OP (*μm*)	Male	50	697.27	10.90
	Female	14	720.71	14.14

The table shows slight differences in microstructural measurements between male and female samples.

Table 13 Independent sample t-test of microstructural measurements between male and female bone thin sections.

	OC	*HCD*	*HCA*	*HCP*	*HLC*	*CT*	*MCD*	*OD*	*OA*	*OP*
t	0.57	-0.96	-0.29	-0.05	-0.11	1.22	0.27	-1.05	-1.10	-1.07
df	62	62	62	62	62	62	62	62	62	62
Sig. (2-tailed)	0.57	0.34	0.78	0.96	0.91	0.23	0.79	0.30	0.27	0.29

The table shows no significant difference in microstructural measurements between male and female samples.

4.3 Human age estimation

By using the *K-S* test, microstructural measurements in human bone showed a normal data distribution (Table 14). The Pearson correlation test showed that *MCD* ($P < 0.05$) and *OP*, *OD*, *OA* and *OC* ($P < 0.01$) have significant correlations with age (Table 15). The osteon count showed the highest correlation with age ($R = 0.43$), followed by osteon diameter ($R = 0.42$), osteon perimeter ($R = 0.34$), and osteon area ($R = 0.32$).

Table 14 Kolmogorov-Smirnov test for microstructural parameters in human bone thin sections.

	OC	*HCD*	*HCA*	*HCP*	*HLC*	*CT*	*MCD*	*OD*	*OA*	*OP*
N	64	64	64	64	64	64	64	64	64	64
Kolmogorov-Smirnov	1.02	.94	1.29	1.15	.67	.89	1.07	.62	.78	.69
Asymp. *Sig.* (2-tailed)	.243	.332	.070	.141	.753	.403	.198	.825	.570	.723

a Test distribution is Normal.
b Calculated from data.
The table shows normal data distribution (significance level more than 0.05).

Table 15 Pearson correlation analysis between age and microstructural parameters.

	OC	*HCD*	*HCA*	*HCP*	*HLC*	*CT*	*MCD*	*OD*	*OA*	*OP*
Pearson Correlation	.43**	.15	.07	.02	.08	.10	.27*	-.42**	-.32**	-.34**
Sig. (2-tailed)	.000	.232	.571	.840	.524	.409	.030	.000	.008	.006
N	64	64	64	64	64	64	64	64	64	64

**** P < 0.01**
*** P < 0.05**

In this study, *OC* showed positive correlation with age, while *OD*, *OA* and *OP* showed negative correlations with age (Table 15). This means that smaller osteons in human bone has allowed more osteons to exist in the cortical bone. Haversian canal parameters such as *HCA*, *HCD* and *HCP* showed positive correlations with age, which means that larger Haversian canals are present in cortical bone. Young osteons usually have large Haversian canals (Junqueira and Carneiro, 2005), which indicate that more osteons were formed with increasing age.

In this study, there were 9 diabetic patients from 64 human samples. The microstructural measurements showed only slight differences between the diabetics and healthy individuals in the descriptive statistics (Table 16). By using the independent sample *t*-test (Table 17), the microstructural measurements showed no significant difference between diabetic patients and healthy individuals, and thus, the null hypothesis was accepted. This showed that the presence of diabetes mellitus in human did not affect the bone microstructures.

Table 16 Descriptive statistics of microstructural parameters for diabetes mellitus (*DM*) and non-*DM* in human bone thin sections.

Parameter		*N*	Mean ± *SEM*
OC (*ct*/μm^2)	*DM*	9	14.69 ± 1.84
	Non-*DM*	55	14.54 ± 0.56
HCD (μm)	*DM*	9	51.30 ± 2.94
	Non-*DM*	55	49.83 ± 0.97
HCA (μm^2)	*DM*	9	218.2 ± 22.48
	Non-*DM*	55	191.77 ± 8.39
HCP (μm)	*DM*	9	186.03 ± 9.63
	Non-*DM*	55	175.84 ± 3.40
HLC (*ct*/osteon)	*DM*	9	6.15 ± 0.55
	Non-*DM*	55	5.87 ± 0.26
CT (*mm*)	*DM*	9	5.39 ± 0.69
	Non-*DM*	55	4.81 ± 0.15
MCD (*mm*)	*DM*	9	11.50 ± 1.17
	Non-*DM*	55	9.80 ± 0.38
OD (μm)	*DM*	9	192.57 ± 7.11
	Non-*DM*	55	200.77 ± 2.42
OA (μm^2)	*DM*	9	313.65 ± 24.52
	Non-*DM*	55	336.00 ± 9.31
OP (μm)	*DM*	9	672.86 ± 26.99
	Non-*DM*	55	707.23 ± 9.57

The table shows that slight differences in microstructural measurements between diabetics and non-diabetics.

Table 17 Independent sample t-test between *DM* and non-*DM* in human bone thin sections.

	OC	*HCD*	*HCA*	*HCP*	*HLC*	*CT*	*MCD*	*OD*	*OA*	*OP*
t	0.09	0.54	1.16	1.10	0.39	1.24	1.60	-1.23	-0.89	-1.32
df	62	62	62	62	62	62	62	62	62	62
Sig. (2-tailed)	0.92	0.58	0.24	0.27	0.69	0.21	0.11	0.22	0.37	0.19

The table shows no significant differences in microstructural measurements between *DM* and non-*DM*.

Two cases numbered 17 and 48 were found to be residuals by using the 'casewise diagnostics test for residuals' (Table 18). Cases numbered 17 and 48, were elderly female

aged 91 and 90 years old, respectively (Appendix 1). The scatterplots showed a good scatter of data after removing the residuals from the data sample (Figure 20).

Table 18 Casewise diagnostics in regression analysis for human bone thin sections.

Case Number	age	Residual
17	91.00	41.02
48	90.00	37.23

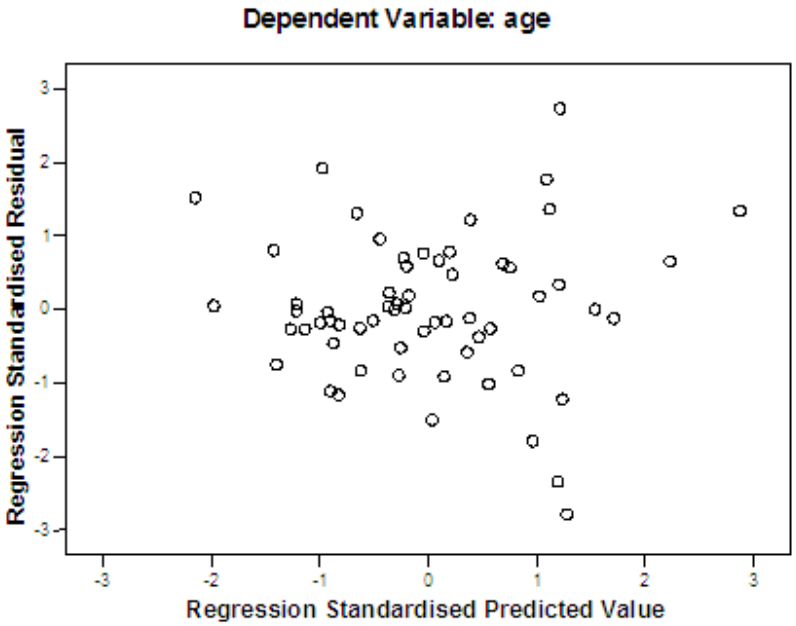

Figure 20 Scatterplot for regression analysis of parameters in human bone thin sections after removal of residuals.

The microstructural measurements were analysed by using stepwise regression analysis to produce age regression equations by using various combinations of the 10 parameters. The results showed three age equations (Table 19), and the third equation was chosen as it showed the highest multiple correlation coefficient (R^2) of 0.355 with the least standard error of estimate (*SEE*) of 10.41 years ($P < 0.01$). The R^2 of 0.355 represented the coefficient variation, which showed that only 35.5% of the variation in age was attributed

to microstructural parameters, while the remaining 64.5% was due to random error such as different types of human races, animal species and types of bones. The standard error of estimate of 10.41 years indicated that the mean of age estimate is estimated to lie between ±10.41 years.

Estimated age (years) = 46.972 + 0.913 (*OC*) – 0.255(*OD*) + 0.624 (*HCD*)

Table 19 Age regression equations derived from stepwise regression analysis.

Equation	*Multiple R^2*	*SEE*
$Y = 99.38 - 0.295\ OD$	0.18*	11.48
$Y = 84.84 - 0.362\ OD + 0.558\ HCD$	0.28*	10.85
$Y = 46.97 - 0.255\ OD + 0.624\ HCD + 0.913\ OC$	0.355*	10.41

***P* < 0.01**

The regression equation was validated against the study sample. The difference between known age and estimated age showed age ranges from -28.48 to + 28.98 years in male, and age ranges from -44.29 to +24.35 years in female samples (Table 36 – Appendix 3). The difference between the means of known age and estimated age was 0.99 years for male and 4.02 years for female samples (Table 20). The mean difference in ages in human male and female did not show any significant difference by using the independent sample *t*-test (Table 21). This indicated that the age regression equation has produced good approximation of ages for the human sample in this study.

Table 20 Descriptive statistics of mean known and estimated age for male and female bone thin sections.

		N	Mean	*SD*	*SEM*
Known age	Male	50	41.68	11.85	1.67
	Female	14	43.00	24.36	6.51
Estimated age	Male	50	40.79	6.91	0.97
	Female	14	39.98	9.78	2.61

The table shows only slight difference between known and estimated ages in male and female.

Table 21 Independent sample *t*-test between known and estimated age in male and female bone thin sections.

	t	*df*	Sig. (2-tailed)
Known age	-0.009	28	0.993
Estimated age	0.93	28	0.359

The table shows no significant difference between known and estimated ages in male and female.

In this study, three age regression equations were produced for tibia, femur and humerus. (Table 22). The equation for tibia showed the highest correlation with age (R = 0.82), followed by femur (R = 0.77) and humerus (R = 0.42). The R^2 of 0.18 in the regression equation in humerus showed that 18% of variation in age in humerus was attributed to microstructural measurements, while the remaining 82% of variation in age was due to random error such as different human races and sex. Nevertheless, tibia and femur bones have shown good coefficient variation of 67% and 59%, respectively. This means that 67% of variation in age in tibia was attributed to microstructural measurements, given the fact that they are derived from different human races and sex.

Table 22 Regression formulas based on microstructural parameters for different types of bone.

Bone type	Regression equations	*R*	R^2	*SEE*	*Sig.*
Humerus	*Y*= 21.73 + 1.12 (*OC*)	0.42	0.18	11.01	0.05*
Tibia	*Y*= 158.39 - 15.15 (*CT*)	0.82	0.67	12.28	0.05*
Femur	*Y*= 6.13 + 2.95 (*OC*)	0.77	0.59	14.04	0.05*

***P* < 0.05**

This table shows that the regression equation for tibia has the highest multiple correlations (R^2), while regression equation for humerus has the lowest *SEE*.

Additionally, two regression equations were produced for male and female samples (Table 23). The equation for female sample showed a higher correlation with age (*R*= 0.79) than in male (*R*= 0.41). Additionally, male samples showed weak coefficient variation (R^2 = 0.17) compared to female samples (R^2 = 0.63). This means that in female samples, 63% of variation in age was attributed to microstructural measurements, while the remaining 37% variation in age was due to random error. Although the number of male samples (*n* = 50) predominates in this study compared to female (*n* = 14), the results have shown a good coefficient variation for female. There is no explanation to be offered for the above result to occur in female samples, which may need further research to explore such findings.

Table 23 Regression formulas based on microstructural parameters for male and female thin bone sections.

Sex	Regression equations	*R*	R^2	*SEE*	*Sig.*
Male	*Y*= 25.06 + 1.12 (*OC*)	0.41	0.17	10.94	0.01*
Female	*Y*= -10.51 + 5.43 (*MCD*)	0.79	0.63	15.43	0.001**

***P* < 0.01**

****P* < 0.001**

The table shows that the regression equation for female has the highest multiple correlations (R^2).

4.4 Observational error analysis

Analysis of *OC* showed values ranged from 42 (slide no. 7) to 2 (slide no. 9) by the first observer and the third observer, respectively (Table 24 and Table 25). The value of *OC* varied from 17 to 42 in slide no. 7, and the value of *OC* varied from 2 to 17 in slide no. 9. By using paired *t*-test, *OC* values in the first and seventh day showed significant difference in the second observer ($P < 0.01$) (Table 26). By using the *ANOVA* test, there were no significant differences in *OC* between the three observers (Table 27).

Table 24 Osteon count 1 and 2 for observers 1, 2 and 3.

	Observer 1		Observer 2		Observer 3	
Sample	*OC1*	*OC2*	*OC1*	*OC2*	*OC1*	*OC2*
1	14.00	16.00	24.00	10.00	10.00	16.00
2	25.00	26.00	30.00	22.00	26.00	21.00
3	26.00	21.00	18.00	17.00	17.00	14.00
4	13.00	17.00	4.00	2.00	5.00	11.00
5	19.00	13.00	13.00	10.00	12.00	13.00
6	31.00	30.00	33.00	25.00	25.00	24.00
7	42.00	28.00	30.00	17.00	21.00	18.00
8	30.00	30.00	36.00	25.00	37.00	28.00
9	12.00	17.00	12.00	9.00	3.00	2.00
10	23.00	16.00	18.00	22.00	14.00	23.00

Table 25 Descriptive statistics of *OC* 1 and *OC* 2 for the three observers.

Observer 1/2/3			Mean	*N*	*SD*
1	Pair 1	*OC1*	23.5	10	9.44
		OC2	21.4	10	6.5
2	Pair 2	*OC1*	21.8	10	10.46
		OC2	15.9	10	7.84
3	Pair 3	*OC1*	17	10	10.46
		OC2	17	10	7.53

This table shows slight differences in *OC* between the first and seventh day in the three observers.

Table 26 Paired sample *t*-test between the observers in osteon counting.

	t	*df*	Sig. (2-tailed)
Pair 1 *OC1-OC2*	1.13	9	0.28
Pair 2 *OC1-OC2*	3.20	9	0.01*
Pair 3 *OC1-OC2*	0	9	1.00

*** *P* < 0.01**

Table 27 One-way analysis of variance (*ANOVA*) of the mean *OC* between the three observers.

	df	*F*	Sig.
Between groups	2	1.09	0.35
Within groups	27		
Total	29		

5. DISCUSSION

5.1 Human and nonhuman bone microstructure

The research question has focused on the examination of microstructural parameters, which can be used for the identification of human and nonhuman in skeletal remains. In this study, ten microstructural parameters namely, *CT*, *MCD*, *OC*, *OD*, *OA*, *OP*, *HCD*, *HCA* and *HCP* were measured in 64 human and 65 nonhuman bone samples. The microstructural measurements showed significant differences between human and non-human bone thin sections ($P < 0.001$), consistent with those in the literature (Cattaneo *et al*., 1999; Jowsey, 1966; Martiniaková *et al*., 2006; Muller and Demarez, 1993; Owsley *et al*., 1985). This study has obtained a high classification rate by using discriminant function analysis. Cross validation of the equation on the sample showed correct classification rates for 79.1% of cases, higher than that (76.2%) in the literature (Martiniaková *et al*., 2006).

Previous studies have shown that as animals increase in size, their microstructural parameters will increase in size up to the size of a human (Jowsey, 1966; Stout and Ross, 1991), and become constant after a certain size is reached (Jowsey, 1966). Jowsey (1966) reported that the mean osteon diameter was the smallest in rabbit, followed by monkey, human and cow (Table 28), and this study has shown results comparable with those reported by Jowsey (1966).

\

Table 28 Mean *OD* and *HCP* in human and animals in Jowsey (1966) and this study.

Samples	Jowsey (1966)			This study (2006)		
	n	Mean *OD* (μm)	Mean *HCP* (μm)	*n*	Mean *OD* (μm)	Mean *HCP* (μm)
Human	26	223	173	64	198	177
Rabbit	6	92	54	1	122	94
Monkey	2	216	85	1	180	199
Cow	4	250	213	9	181	124

This table shows comparable values of mean *OD* and *HCP* in Jowsey (1966) and this study.

Literature also showed that microstructural measurements were useful to identify human and animal skeletal remains. In this study, the values of *OC* and *HCD* were found to be higher in human than those in deer, which is in agreement with those reported by Owsley *et al*. (1985). Also, in this study, the value of *OC* was comparable with that reported by Iwaniec *et al.* (1998) (Table 29).

Table 29 Microstructural measurements of human and deer in Owsley *et al.* (1985), Iwaneic and Crenshaw (1998) and this study.

Parameter (mean)	Owsley *et al*. (1985)		(Iwaniec *et al*., 1998)	This study (2006)	
	Human (n = 1)	Deer (n = 1)	Human (n = 94)	Human (n = 64)	Deer (n = 6)
CT (*mm*)	3.75	3.3	-	4.9 ±1.29	3.44
OC (ct/mm^2)	5.92	1.055	16.6 ± 4.7	14.57 ± 4.37	10.01
HCD (μm)	175	71	-	50.05 ±7.4	43.68

The above results showed that histologic method is the best method to be used in the identification of human and nonhuman bone. Other method such as immunologic method was not used in this study due to the fact that the protein content in bone may sometimes be altered or has been poorly preserved, and this will affect the final results. Similarly, *DNA* and *RNA* analyses were also not used because the results need to be compared with those from close relatives or family members, who often do not have *DNA* analysed

beforehand. Combination with other method such 4th rib histologic method may help narrow down the search for individuals for identification purposes.

The fact that more animal bones have been mistaken for human in several medicolegal cases, have brought significant implications in the assessment of animal species and the choice of animals to be sampled for identification purposes. Future research will need to consider the edible animals such as cows, goats and pig as they are often found in human inhabitants. Nevertheless, wild animals such as tigers, bears and primates will also be considered for skeletal remains that are found in the woods or jungle. Thus, the choice of animal species is important to complement the research study to form a database collection of various animals.

5.2 Human male and female bone microstructure

In this study, the microstructural measurements in male and female samples did not show any significant difference. This was in agreement with that in the literature (Dupras and Pfeiffer, 1996; Pfeiffer, 1998), which showed that there was no significant difference between male and female samples in microstructural measurements (Table 30).

Table 30 Osteon count for male and female in Pratte and Pfeiffer (1999) and this study.

Parameter		(Pratte and Pfeiffer, 1999)	(This study, 2006)
OC			
(Mean ± *SD*)	Total (*N*)	15.01 ± 3.26 (62)	14.57 ± 4.37 (64)
	Male (*N*)	14.46 ± 3.15 (38)	14.74 ± 4.26 (50)
	Female (*N*)	15.76 ± 3.28 (24)	13.98 ± 4.85 (14)

The table shows *OC* in male and female were comparable between Pratte and Pfeiffer (1999) and this study.

However, in other studies (Burr *et al*., 1990; Mulhern and Gerven, 1997; Thompson, 1980; Thompson and Gunness-Hey, 1981), microstructural measurements have been

shown to be significantly different between male and female samples. Literature (Thompson, 1980) showed that cortical bone was found to be thinner in female than in male in aged people ($P < 0.001$), which is in agreement to what has been found in this study, although the results were not significant.

Additionally, female bone showed fewer osteons ($P < 0.001$) than do males due to the presence of larger osteons ($P < 0.05$), and thinner cortical bone in female (Mulhern and Gerven, 1997). These findings were in agreement with this study, in which females have fewer osteons and larger osteons (Table 31). Further, Haversian canals were larger in female than in the male ($P < 0.05$) (Thompson and Gunness-Hey, 1981), which were also in agreement with this study.

Table 31 Mean *OC*, *OA* and *OD* in Mulhern and Gerven (1997) and this study (2006).

		Mulhern and Gerven (1997)		This study (2006)	
Parameter		*n*	Mean	*n*	Mean ± *SE*
OC	Male	19	9.74 / mm^{2**}	50	14.74 ± 0.6 / μm^2
	Female	24	6.73 / mm^{2**}	14	13.98 ± 1.3 / μm^2
OA	Male	19	0.034 mm^{2*}	50	327.77 μm^2
	Female	24	0.038 mm^{2*}	14	351.05 μm^2
OD	Male	19	0.206 *mm**	50	198.34 μm
	Female	24	0.219 *mm**	14	204.20 μm

*** *P* < 0.05**
****P* < 0.0001**
This table shows fewer osteons and larger osteons in female than in male in Mulhern and Gerven (1997) and this study.

5.3 Human age estimation

The research question has focused on the examination of microstructural parameters that can be used to determine age estimation in human population, particularly in Kuala Lumpur, Malaysia. In this study, ten microstructural parameters such as *CT*, *MCD*, *OC*,

OD, *OA*, *OP*, *HCD*, *HCA* and *HCP* were measured in 64 human bone samples for age estimation. From the age regression equation, age estimation in human has shown standard error of estimates comparable with those in the literature (Ericksen, 1991; Yoshino *et al*., 1994) (Table 32; Table 33). The correlation test showed that *OC* and *HCD* have positive correlations with age, while *OD* has negative correlation with age. This means that there were more osteons, larger Haversian canals and smaller osteons with advancing age, consistent with increased remodelling process in aged people, whereby more osteons will be produced in cortical bone, and new osteons usually have large Haversian canals (Junqueira and Carneiro, 2005).

When the equation was tested against the study sample, male samples showed closer approximation of ages than in female. In this study, the regression equation showed correlation coefficient and standard error of estimates (*SEE*), which were comparable with those in the literature (Narasaki, 1990) (Table 34). Regression equations produced for different types of bone have also shown comparable values of R^2 (coefficient variation) and *SEE* with those in in the literature (Stout and Stanley, 1991) (Table 35).

Table 32 Age regression equations by Yoshino *et al.* (1994) and this study.

	Parameter	Regression equation	*R*	R^2	*SEE*
(Yoshino et al., 1994)	*OC*	5.72+ 2.89 (*OC*)	0.58*	-	9.28
(This study, 2006)	*OC, OD and HCD*	46.97+0.91(*OC*)–0.25(*OD*)+0.62 (*HCD*)	0.6**	0.36	10.41

***P* < 0.01**

**** P* < 0.001**

This table shows comparable values of '*R'* and '*SEE'* in the regression equations by Yoshino *et al.* (1994) and this study.

Table 33 Age regression equations in Kerley (1965), Singh and Gunberg (1969), Thompson (1979), Ericksen (1991) and this study.

	Regression equation	*R*	R^2	*SEE*	*Sig.*
(Kerley, 1965)	57.811- 1.728*X*+ 0.013 X^2	0.815	-	13.85	-
(Singh and Gunberg, 1970)	89.01- 0.62X^3	0.937	-	3.82	0.05
(Thompson, 1979)	28.978+ 128.557X^1 – 1.79X^2– 7.543X^3– 7.633X^4+ 2.688X^5	0.862	-	7.06	-
(Ericksen, 1991)	92.42+ 1.07X^1+ 2.5X^2+ 0.25X^3+ 0.3X^4- 1.52X^5- 0.57X^6- 0.61X^7- 0.35X^8	0.67	-	10.08	-
(Stout, 1986)	-12.239+ 2.873 (*TOC*)	0.682	-	-	-
(This study, 2006)	30.21+ 1.125 (*OC*)- 0.053 (*OP*)+ 0.623 (*HCD*)	0.578	0.334	10.59	0.001

Note that the parameters for Stout (1986) were *TOC* (total osteon count).
The parameters for Ericksen (1991) were X^1(*OC*), X^2 (type II osteon), X^3(fragment), X^4 (resorption spaces), X^5(primary canal), X^6(mean percent unremodeled bone), X^7 (mean percent osteonal bone), and X^8(mean percent fragmental bone).
The parameters for Thompson (1979) were X^1(*HLC* and *HCA*), X^2(*CT*), X^3(*OP*/*OC*), X^4 (total *OP*), X^5(*OC*).
The parameter for Singh and Gunberg (1970) was X^3(mean *HCD*). The parameters for Kerley (1965) were *X* (*OC*) and X^2(osteon fragment count).
This table shows comparable values of '*R*' and '*SEE*' in the regression equations by Kerley (1965), Thompson (1979), Ericksen (1991) and this study. The regression equation by Singh and Gunberg (1969) showed the highest correlation '*R*' with age.

Table 34 Regression equations for male and female samples for Narasaki (1990) and this study.

	Sex	Regression equation	*R*	R^2	*SEE*
(Narasaki, 1990)	Male	257.77+ 2.017*CT*- 14.6*CW*- 0.017T*OC*+ 7754*MOA*- *1670OASD*- 509.7*MOP*- 125.9O*PSD*- 44.89*TOA*	0.581	-	9.28
	Female	67.18+ 2.194*CT*- 407*CW*- 1.875*TOC*- 7162*MOA*+ 6103O*ASD*+ 278.5*MOP*- 427.3*OPSD*+ 191.2*TOA*	0.748	-	9.95
(This study, 2006)	Male	*Y*= 25.06 + 1.12 (*OC*)	0.41	0.17	10.94
	Female	*Y*= -10.51+ 5.43 (*MCD*)	0.79	0.63	15.43

Note that the parameters for Narasaki (1990) were *CT* (cortical thickeness), *CW* (core weight), *TOC* (total osteon count),
MOA* (mean osteon area), *OASD* (osteon area standard deviation), *MOP* (mean osteon perimeter, *OPSD
(osteon perimeter standard deviation), *TOA* (total osteon area).
This table shows comparable values of '*R*' and '*SEE*' in male and female regression equations by Narasaki (1990) and this study.

Table 35 Regression equation for tibia by Stout and Stanley (1991) and this study (2006).

	Bone type	Regression equation	R^2	*SEE*
Stout and Stanley (1991)	Tibia	14.81+ 2.37 (*TOC*)	0.41	14.86
This study (2006)	Tibia	158.39+15.15 (*CT*)	0.67	12.28

This table shows comparable values of 'R^2' and '*SEE*' in regression equation for tibia by Stout and Stanley (1991) and this study (2006).

The fact that age estimation in this study has shown good approximation of ages in comparison with other studies is promising. Nevertheless, the results have to be taken with caution, as different bones were sampled in this study, and different bones may undergo different types of stresses and strains resulting in changes in the morphologic structure of the bone. In this study, posteromedial and posterolateral locations have been chosen to avoid the linea aspera in posterior location, as this location may show the most variation in microstructural measurements in femur. Unfortunately, these locations have also been applied to all other bones in this study with the assumption that they are also applicable to other bones. In future, sampling locations in other bones have to be considered so that bony ridges in each type of bone could be avoided, as these locations may cause variation in their microstructural measurements.

5.4 Observational error analysis

In this study, the inter-observer analysis did not show any significant difference in *OC* between three different observers. These findings were in agreement with those in the literature (Baccino *et al*., 1999; Lynnerup *et al*., 1998), which means that identification of osteon can be done, even with limited experience. The identification of an osteon is usually based on the presence of a cement line around an osteon, which has to be

identified to be able to distinguish an osteon from a primary osteon, which do not have a cement line.

6. CONCLUSION AND RESEARCH IMPLICATIONS

This study has produced discriminant functions for human and nonhuman based on six microstructural parameters that is, *HCA*, *HLC*, *OP*, *OC*, *HCD* and *HCP*, and achieved a high classification rate for human and nonhuman identification. This study has thus, achieved its aims and objectives to identify human and nonhuman by analysing the microstructural parameters in human and nonhuman bone thin sections, as well as, age estimation in human population in Kuala Lumpur by analysing the microstructural parameters in human bone thin sections. This study has produced age regression equations for human sample population in Kuala Lumpur area, and a standard error of estimate (*SEE*), which was comparable with those in the literature. Additionally, cross validation against the study sample showed close approximation of ages between known and estimated ages in the human samples.

In conclusion, this study has achieved both its aims and objectives to perform human and nonhuman identification and age estimation in human bone by the assessment of microstructural parameters in bone thin sections. The results from this study will have significant implications in the assessment of fragmentary skeletal remains and forensic population samples for identification purposes.

7. BIBLIOGRAPHY

Aeillo LC, and Molleson T (1993) Are microscopic ageing techniques more accurate than macroscopic ageing techniques? *Journal of Archaeological Science 20:*689-704.

Angel JL (1974) Bones can fool people. *FBI Law Enforcement Bulletin 43:*17-20.

Anonymous (2009) http://images.search.yahoo.com/search/images?p=Malaysia+map.

Baccino E, Ubelaker DH, Hayek LAC, and Zerilli A (1999) Evaluation of seven methods of estimating age at death from mature human skeletal remains. *Journal of Forensic Sciences 44:*931-936.

Beckett S, and Rogers K (2006) A new method of accurate species discrimination from bone fragments. *8th Annual BAHID Meeting, Human Identification: An international perspective.*

Bellis C, Ashton KJ, Freney L, Blair B, and Griffiths LR (2003) A molecular genetic approach for forensic animal species identification. *Forensic Science International 134:*99-108.

Bender K, Schneider PM, and Rittner C (2000) Application of mtDNA sequence analysis in forensic casework for the identification of human remains. *Forensic Science International 113:*103-107.

Black J, Mattson R, and Korostoff E (1974) Haversian osteons: size, distribution, internal structure and orientation. *Journal of Biomedical Material Research 8:*299-319.

Blackett RS, and Keim P (1992) Big game species identification by deoxyribonucleic acid (DNA) probes. *Journal of Forensic Sciences 37:*590-596.

Bland M (1995) *An Introduction to Medical Statistics.* Oxford: Oxford University Press.

Burr DB, Ruff CB, and Thompson DD (1990) Patterns of skeletal histologic change through time: a comparison of an archaic Native American population with modern populations. *Anatomical Record 226:*307-313.

Butler JM, and Levin BC (1998) Forensic applications of mitichondrial DNA. *Tib Tech 16:*158-162.

Carter PH, and Schipani E (2006) The roles of parathyroid hormone and calcitonin in bone remodeling: prospects for novel therapeutics. *Endocr Metab Immune Disord Drug Targets 6:*59-76.

Cattaneo C, DiMartino S, Scali S, Craig OE, Grandi M, and Sokol RJ (1999) Determining the human origin of fragments of burnt bone: a comparative study of histological, immunological and DNA techniques. *Forensic Science International 102:*181-191.

Chilvaquer I, Katz JO, Glassman DM, Prihoda TJ, and Cottone JA (1987) Comparative radiographic study of human and animal long bone patterns. *Journal of Forensic Sciences 32:*1645-1654.

Cho H, Stout SD, Madsen RW, and Streeter MA (2002) Population-specific histological age-estimating method: a model for known African-American and Europian-American skeletal remains. *Journal of Forensic Sciences 47:*12-18.

Cormack DH (1987) *Ham's Histology*. Philadelphia: J. B. Lippincott.

Cruz C, Ribeiro T, Viera_Silva C, Lucas I, Geada H, and Espinheira R (2004) Identification by mtDNA of exchanged human body remains. *International Congress Series 1261:*374-376.

Cuijpers AGFM, and Schutkowski H (1993) Histological age determination of the cremated human bones from the urnfields of Deventer-`T Bramelt and Markelo Friezenberg. *Helinium XXXIII/I:*99-107.
Dix JD, Stout SD, and Mosley J (1991) Bones, blood, pellets, glass and no body. *Journal of Forensic Sciences 36:*949-952.
Dupras TL, and Pfeiffer SK (1996) Determination of sex from adult human ribs. *Canadian Society of Forensic Science Journal 29:*221-231.
Enlow DH (1963) *Principles of Bone Remodelling*. Springfield: Thomas.
Enlow DH, and Brown SO (1956) A comparative histological study of fossil and recent bone tissues, part I. *Texas Journal of Science 7:*405-443.
Enlow DH, and Brown SO (1957) A comparative histological study of fossil and recent bone tissues, part II. *Texas Journal of Science 9:*186-214.
Enlow DH, and Brown SO (1958) A comparative histological study of fossil and recent bone tissues, part III. *Texas Journal of Science 9:*187-230.
Ericksen MF (1980) Patterns of microscopic bone remodeling in three aboriginal American populations. In DL Browman (ed.): *Early Native Americans: Prehistoric Demography, Economy and Technology*. The Hague: Mouton, pp. 239-270.
Ericksen MF (1991) Histologic estimation of age at death using the anterior cortex of the femur. *American Journal of Physical Anthropology 84:*171-179.
Eriksen EF, and Langdahl B (1995) Bone remodelling and its consequences for bone structure. In A Odgaard and H Weinans (eds.): *Bone Structure and Remodelling*. River Edge: World Scientific, pp. 25-36.
Frost HM (1973) *Bone Remodeling and its Relationship to Metabolic Bone Diseases, (Volume III)*. Springfield: Charles C. Thomas.
Frost HM (1987a) Secondary osteon population densities: an algorithm for estimating the missing osteons. *Yearbook of Physical Anthropology 30:*239-254.
Frost HM (1987b) Secondary osteons population: an algorithm for determining mean bone tissue age. *Yearbook of Physical Anthropology 30:*221-238.
Frost HM (1990) Skeletal structural adaptations to mechanical usage (SATMU). 2. Redefining Wolff's law: The bone modelling problem. *Anatomical Record 226:*413-414.
Geneser F (1986) *Textbook of Histology*. Copenhagen: Munksgaard.
Gilbert BM (1980) *Mammalian Osteology*. Laramie, Wyoming: B. Miles Gilbert.
Guglich EA, Wilson PJ, and White BN (1994) Forensic application of repetitive DNA markers to the species identification of animal tissues. *Journal of Forensic Sciences 39:*353-361.
Ham AW, and Cormack DH (1979) *Histophysiology of Cartilage, Bone and Joints*. Philadelphia: JB Lippincott.
Hoffman JM (1984) Identification of nonskeletonized bear paws and human feet. In TA Rathbun and JE Buikstra (eds.): *Human Identification: Case Studies in Forensic Anthropology*. Illinois: Thomas, pp. 96-106.
Imaizumi K, Saitoh K, Sekiguchi K, and Yoshino M (2002) Identification of fragmented bones based on anthropological and DNA analyses: case report. *Legal Medicine 4:*251-256.

Iwaniec UT, Crenshaw TD, Shoeninger MJ, Stout SD, and Ericksen MF (1998) Methods for improving the efficiency of estimating total osteon density in the human anterior mid-diaphyseal femur. *American Journal of Physical Anthropology 107:*13-24.

Jowsey J (1966) Studies of haversian systems in man and some animals. *Journal of Anatomy 100:*857-864.

Junqueira LC, and Carneiro J (2005) *Basic Histology: Text and Atlas*. New York: McGraw-Hill.

Kerley ER (1965) The microscopic determination of age in human bone. *American Journal of Physical Anthropology 23:*149-164.

Lynnerup N, Frohlich B, and Thomsen JL (2006) Assessment of age at death by microscopy: unbiased quantification of secondary osteons in femoral cross sections. *Forensic Science International 159S.*

Lynnerup N, Thomsen JL, and Frohlich B (1998) Intra- and inter-observer variation in histological criteria used in age at death determination based on femoral cortical bone. *Forensic Science International 91:*219-230.

Marieb EN (2001) *Human Anatomy and Physiology*. San Francisco: Benjamin Cummings.

Martin RB, and Burr DB (1989) *Structure, Function and Adaptation of Compact Bone*. New York: Raven Press.

Martin RB, Burr DB, and Sharkey NA (1998) *Skeletal Tissue Mechanics*. New York: Springer-Verlag.

Martiniaková M, Grosskopf B, Omelka R, Vondráková M, and Bauerová M (2006) Differences among species in compact bone tissue microstructure of mammalian skeleton: use of a discriminant function analysis for species identification. *Journal of Forensic Sciences 51:*1235-1239.

Martrille L, Ubelaker DH, Cattaneo C, Seguret F, Tremblay M, and Baccino E (2007) Comparison of four skeletal methods for the estimation of age at death on white and black adults. J*ournal of Forensic Sciences 52:*302-307.

Miller ME, Christensen GC, and Evans HE (1964) *Anatomy of the Dog*. Philadelphia: WB Saunders.

Mulhern DM, and Gerven DPV (1997) Patterns of femoral bone remodeling dynamics in a medieval Nubian population. *American Journal of Physical Anthropology 104:*133-146.

Mulhern DM, and Ubelaker DH (2001) Differences in osteon banding between human and nonhuman bone. *Journal of Forensic Sciences 46:*220-222.

Muller M, and Demarez R (1993) Cited in: Harsanyi. In G Grupe and AN Garland (eds.): *Histology of Ancient Bone: Methods and Diagnosis*. Berlin: Springer-Verlag, pp. 80-94.

Murad TA, and Boddy MA (1987) A case with bear facts. J*ournal of Forensic Sciences 32:*1819-1826.

Naito E, Dewa K, Ymanouchi H, and Kominami R (1992) Ribosomal ribonucleic acid (rRNA) gene typing for species identification. *Journal of Forensic Sciences 37:*396-403.

Narasaki S (1990) Estimation of age at death by femoral osteon remodeling: Application of Thompson's core technique to modern Japanese. *Journal Anthropology Society Nippon 98:*29-38.
Owsley DW, and Mann RW (1990) Medicolegal case involving a bear paw. *Journal of American Podiatric Medical Association 80:*623-625.
Owsley DW, Mires AM, and Keith MS (1985) Case involving differentiation of deer and human bone fragments. *Journal of Forensic Sciences 30:*572-578.
Parfitt AM (1984) The cellular basis of bone remodelling: the quantum concept re-examined in light of recent advances in the cell biology of bone. *Calcified Tissue International 36:*S37-S45.
Parfitt AM (1996) Hormonal influences in bone remodeling and bone loss: application to the management of primary hyperparathyroidism. *Annals of Internal Medicine 125:*413-415.
Pfeiffer S (1998) Variability in osteon size in recent populations. *American Journal of Physical Anthropology 106:*219-227.
Pirok DJ, Ramser JR, Takahashi H, Villanueva AR, and Frost HM (1966) Normal histological, tetracycline and dynamics parameters in human, mineralised bone sections. *Henry Ford Hospital Medical Bulletin 14:*195-218.
Pollitzer WS, and Anderson JJB (1989) Ethnic and genetic differences in bone mass: a review with a hereditary vs environmental perspective. *American Journal Clinical Nutrition 50:*1244-1259.
Pratte DG, and Pfeiffer S (1999) Histological age estimation of a cadaveral sample of diverse origins. *Canadian Society Forensic Science Journal 32:*155-167.
Raisz LG (1999) Physiology and pathophysiology of bone remodelling. *Clinical Chemistry 45:*1353-1358.
Robling AG, and Stout SD (1999a) Morphology of the drifting osteon. *Cells, Tissues and Organs 164:*192-204.
Samson C, and Branigan K (1987) A new method of estimating age at death from fragmentary and weathered bone. In A Boddington, AN Garland and RC Janaway (eds.): *Death, Decay and Reconstruction: Approaches to Archaeology and Forensic Science.* Manchester: Manchester University Press, pp. 101-107.
Shipman P, Walker A, and Bichell D (1985) *The Human Skeleton*. Cambridge: Harvard University Press.
Singh IJ, and Gunberg DL (1970) Estimation of age at death in human males from quantitative histology of bone fragments. *American Journal of Physical Anthropology 33:*373-382.
SPSS for windows (Version 13.0).
Stout SD (1986) The use of bone histomorphometry in skeletal identification: the case of Francisco Pizarro. *Journal of Forensic Sciences 31:*296-300.
Stout SD (1998) The application of histological techniques for age at death determination. In KJ Reichs and WM Bass (eds.): *Forensic Osteology: Advances in the Identification of Human Remains.* Springfield, Illinois: Charles C Thomas, pp. 237-252.
Stout SD, and Paine RR (1992) Histological age estimation using rib and clavicle. *American Journal of Physical Anthropology 87:*111-115.

Stout SD, and Ross LM (1991) Bone fragments a body can make. *Journal of Forensic Sciences 36:*953-957.
Stout SD, and Stanley SC (1991) Percent osteonal bone versus osteons counts: the variable of choice for estimating age at death. *American Journal of Physical Anthropology 86:*515-519.
Thomas P (1995) *Talking Bones: the Science of Forensic Anthropology*. New York: Facts on File.
Thompson DD (1979) The core technique in the determination of age at death in skeletons. *Journal of Forensic Sciences 24:*902-915.
Thompson DD (1980) Age changes in bone mineralization, cortical thickness and haversian canal area. *Calcified Tissue International 31:*5-11.
Thompson DD (1981) Microscopic determination of age at death in an autopsy series. *Journal of Forensic Sciences 26:*470- 475.
Thompson DD, and Gunness-Hey M (1981) Bone mineral-osteon analysis of Yupik-Inupiaq skeletons. *American Journal of Physical Anthropology 55:*1-7.
Thompson DD, Salter EM, and Laughlin WS (1981) Bone core analysis of Baffin island skeletons. *Arctic Anthropology 18:*87-96.
Thompson TJU (1999) *A Preliminary investigation into the influence of burning on the ability to sex the pelvis.* Master, University of Bradford, Bradford.
Torrey TW, and Feduccia A (1979) *Morphogenesis of the Vertebrates*. New York: John Wiley & Sons.
Ubelaker DH (1999) *Human Skeletal Remains: Excavation, Analysis, Interpretation*. Washington: Taraxacum.
Ubelaker DH, Lowenstein JM, and D.G.Hood (2004) Use of solid-phase double-antibody radioimmunoassay to identify species from small skeletal fragments. *Journal of Forensic Sciences 49:*1-6.
Valente SF, Filippini SE, Santapá OA, Fraga MG, Gagliarda F, Echenique C, and Lonardo AMD (2004) Banco Nacional de Datos Genéticos and human identification of forensic cases. *International Congress Series 1261:*454-456.
Wachter NJ, Krischak GD, Mentzel M, Sarkar MR, Ebinger T, Kinzl L, Claes L, and Augat P (2002) Correlation of bone mineral density with strength and microstructural parameters of cortical bone in vitro. *Bone 31:*90-95.
Walker RA (1990) An assessment of histological age determination techniques (Abstract). *American Journal of Physical Anthropology 81:*313.
Weinbaum S, Cowin SC, and Zeng Y (1994) A model for the excitation of osteocytes by mechanical loading-induced bone fluid shear stresses. *Journal of Biomechanical 27:*339-360.
Weiner S, and Traub W (1991) Organization of crystals in bone. In S Suga and H Nakahara (eds.): *Mechanisms and Phylogeny on Mineralization on Biological Systems.* Tokyo: Springer-Verlag, pp. 246-253.
Welsch U, and Storch V (1976) *Comparative Animal Cytology and Histology*. London: Sidgwick and Jackson.
Wheater PR, and Burkitt HG (1987) *Functional Histology: A Text and Colour Atlas*. Edinburgh: Churchill Livingstone.

Yoshino M, Imaizumi K, Miyasaki S, and Seta S (1994) Histological estimation of age at death using microradiographs of humeral compact bone. *Forensic Science International 64:*191-198.

Appendix 1 Human Samples Catalogue

Catalogue Key

Sex
M = male
F = female
? = unknown

Location
HKL = Hospital Kuala Lumpur
UKMMC = Universiti Kebangsaan Malaysia Medical Centre

Race
Mal = Malay
Chi = Chinese
Ban = Bangladeshi
Ind = Indian
Pak = Pakistani
Indo = Indonesian
Mya = Myanmar

Bone Type
hum = humerus
rad = radius
tib = tibia
uln = ulna
fib = fibula
fem = femur

Types of Injury

hi (fo) = head injury (due to falling object)
mi (fo) = multiple injuries (due to falling object)
mgi = multiple gunshot injuries
mi (fh) = multiple injuries (due to fall from height)
ca = coronary atherosclerosis
asp (ms) = asphyxia (due to manual strangulation)
hi (mva) = head injury (due to motor-vehicle accident)
dm = diabetes mellitus
cai (mva) = chest and abdominal injuries (due to motor vehicle accident)
gi(hc) = gunshot injury (head and chest)
shi(gw) = severe head injury (due to gunshot wound)
ci(mva) = chest injury (due to motor vehicle accident)
hpi(fh) = head and pelvic injuries (due to fall from height)
hci(mva) = head and chest injuries (due to motor vehicle accident)
hi(fh) = head injury (due to fall from height)
mi(mva) = multiple injuries (due to motor vehicle accident)
? = unknown

Number	Sample	Sex	Age	Race	Bone Type	Cause of Death	Origin
1	830.04	*F*	29	*Chi*	*hum*	?	*UKMMC*
2	866.04	*M*	37	*Chi*	*hum*	?	*UKMMC*
3	897.04	*M*	41	*Chi*	*hum*	?	*UKMMC*
4	1009.04	*M*	28	*Chi*	*hum*	?	*UKMMC*
5	1501	*M*	39	*Chi*	*hum*	*cai(mva)*	*UKMMC*
6	bone12	*M*	78	*Chi*	*hum*	?	*UKMMC*
7	boneb	*M*	40	*Ind*	*rad*	?	*UKMMC*
8	cmh	*M*	67	*Chi*	*tib*	?	*UKMMC*
9	335.04	*M*	33	*Mya*	*hum*	?	*UKMMC*
10	997.04	*M*	46	*Chi*	*hum*	*mi (fh)*	*UKMMC*
11	1011.04	*M*	37	*Chi*	*hum*	?	*UKMMC*
12	1012.04	*M*	56	*Chi*	*hum*	*gi (hc)*	*UKMMC*
13	ahmads	*M*	38	*Mal*	*tib*	*dm*	*HKL*
14	bone18	*M*	48	*Chi*	*rad*	?	*UKMMC*
15	bone22	*M*	52	*Chi*	*hum*	?	*UKMMC*
16	bonea	*M*	50	*Chi*	*fem*	?	*UKMMC*
17	csy	*F*	91	*Chi*	*fem*	*dm*	*HKL*
18	f254.03	*M*	26	*Chi*	*rad*	*hi (fo)*	*UKMMC*
19	f255.03	*M*	53	*Ind*	*rad*	*mi (fo)*	*UKMMC*
20	f344.03	*M*	33	*Ind*	*rad*	*mgi*	*UKMMC*
21	f345.03	*M*	32	*Ind*	*rad*	*shi (gw)*	*UKMMC*
22	f479.03	*M*	22	*Chi*	*rad*	*mi (fh)*	*UKMMC*
23	f835.02	*M*	32	*Indo*	*rad*	?	*UKMMC*
24	lowf	*M*	52	*Chi*	*tib*	*dm*	*HKL*
25	nhm	*F*	38	*Mal*	*tib*	*dm*	*HKL*
26	nsh	*F*	31	*Chi*	*fib*	*dm*	*HKL*
27	p995.04	*M*	29	*Ind*	*hum*	?	*UKMMC*
28	samm	*M*	64	*Chi*	*fem*	*dm*	*HKL*
29	bonez	*M*	42	*Chi*	*hum*	?	*UKMMC*
30	cs	*M*	38	*Ind*	*tib*	*dm*	*HKL*
31	f238.03	*M*	40	*Chi*	*rad*	*ci (mva)*	*UKMMC*
32	f377.04	*F*	22	*Chi*	*hum*	*hpi (fh)*	*UKMMC*
33	hu2	*F*	32	*Chi*	*hum*	*hci (mva)*	*UKMMC*
34	hu4	*F*	40	*Chi*	*fem*	?	*UKMMC*
35	hu6	*M*	39	*Chi*	*hum*	?	*UKMMC*
36	hu9	*F*	29	*Chi*	*hum*	*mi (fh)*	*UKMMC*
37	hu10	*M*	49	*Chi*	*fem*	?	*UKMMC*
38	hu15	*F*	25	*Ind*	*hum*	?	*UKMMC*
39	hu18	*M*	39	*Chi*	*hum*	*cai (mva)*	*UKMMC*
40	hu24	*M*	34	*Ind*	*rad*	?	*UKMMC*
41	hu29	*M*	63	*Chi*	*rad*	?	*UKMMC*
42	kaq	*M*	45	*Pak*	*fem*	?	*UKMMC*
43	mka	*F*	48	*Ind*	*tib*	*dm*	*HKL*
44	p651.04	*M*	52	*Chi*	*hum*	?	*UKMMC*
45	p575.04	*M*	37	*Indo*	*fem*	?	*UKMMC*

46	Parthipan	*M*	25	*Ind*	*fem*	*dm*	*HKL*
47	t9562.81	*M*	21	*Chi*	*hum*	?	*UKMMC*
48	wsy	*F*	90	*Chi*	*tib*	*dm*	*HKL*
49	f209.03	*M*	42	*Chi*	*rad*	*ca*	*UKMMC*
50	f229.79	*F*	76	*Chi*	*fem*	?	*UKMMC*
51	f268.03	*M*	52	*Chi*	*rad*	?	*UKMMC*
52	f308.03	*M*	33	*Chi*	*rad*	*asp (ms)*	*UKMMC*
53	f346.03	*M*	38	*Chi*	*rad*	*mgi*	*UKMMC*
54	f366.04	*M*	27	*Ind*	*hum*	*hi (fh)*	*UKMMC*
55	f960.02	*M*	47	*Chi*	*rad*	*hi (mva)*	*UKMMC*
56	f986.02	*M*	50	*Chi*	*hum*	?	*UKMMC*
57	f1362.02	*F*	22	*Indo*	*rad*	*mi (fh)*	*UKMMC*
58	ganesan	*M*	31	*Ind*	*uln*	?	*UKMMC*
59	hu3	*F*	29	*Chi*	*rad*	*shi (gw)*	*UKMMC*
60	hu5	*M*	32	*Chi*	*hum*	*mi (mva)*	*UKMMC*
61	hu11	*M*	40	*Ban*	*rad*	*ca*	*UKMMC*
62	p1010/04	*M*	47	*Chi*	*hum*	?	*UKMMC*
63	p1031.04	*M*	35	*Chi*	*hum*	?	*UKMMC*
64	sami	*M*	53	*Ind*	*fib*	*dm*	*HKL*

Appendix 2 Animal Samples Catalogue

Catalogue Key

Age
Adt = Adult

Origin
MZ = Malacca Zoo
WF = Wild Forest
NZ = National Zoo
But = Butcher
TZ = Taiping Zoo
OF = Ostrich Farm

Cause of Death
pa = Predator's attack
sl = Slaughter
gw = Gunshot wound

Sex
M = Male
F = Female
? = unknown

Bone Type
hum = humerus
rad = radius
tib = tibia
uln = ulna
fib = fibula
fem = femur

Species

bp = black panther (*Panthera pardus*)
blm = banded leaf monkey (*Presbytis femoralis*)
lic = large Indian civet (*Viverra zibetha*)
cpc = common palm civet (*Paradoxurus hermaphroditus*)
ph = pygony hippo (*Cheoropsis liberiensis*)
slm = silver leaf monkey (*Trachypithecus cristatus*)
cow = *Bos indicus*
goat = *Capra hircus*
serow = *Capricornis sumatrensis*
whg = white handed gibbon (*Hylobates lar*)
flc = flat-headed cat (*Prionailurus planiceps*)
mc = malay civet (*Viverra tangalunga*)
rm = rhesus macaque (*Macaca mulatta*)
bd = bawean deer (*Cervus kuhlii*)
ptm = pig-tailed macaque (*Macaca nemestrina*)
deer = *Cervus spp.*
bearcat = *Arctictis binturong*
rabbit = *Oryctolagus cuniculus*
sl = slow loris (*Nycticebus coucang*)
md = mousedeer (*Tragulus javanicus*)
lc = leopard cat (*Prionailurus bengalensis*)
ltm = long-tailed macaque (*Macaca fascicularis*)
gm = greater mousedeer (*Tragulus napu*)
sd = sambar deer (*Cervus unicolor*)
sheep = *Ovis aries*
buffalo = *Bubalus bubalis*

Appendix 2 (contd.)

Sample no.	Sample	Species	Sex	Age	Bone Type	Origin	Cause of Death
65	bpanther65	*bp*	*M*	*Adt*	*Fem*	*MZ*	*pa*
66	c6	cow	*?*	*Adt*	*Hum*	*But*	*sl*
67	an1	deer	*?*	*Adt*	*Rad*	*WF*	*gw*
68	an8	deer	*?*	*Adt*	*Rad*	*WF*	*gw*
69	an13	*blm*	*F*	*Adt*	*Rad*	*NZ*	*pa*
70	an21	sheep	*?*	*Adt*	*Fem*	*But*	*sl*
71	an27	*sd*	*M*	*Adt*	*Fem*	*NZ*	*pa*
72	an28	*rm*	*M*	*Adt*	*Fem*	*NZ*	*pa*
73	an30	goat	*?*	*Adt*	*Fem*	*But*	*sl*
74	an31	deer	*?*	*Adt*	*Rad*	*WF*	*gw*
75	an33	deer	*?*	*Adt*	*Rad*	*WF*	*gw*
76	an34	deer	*?*	*Adt*	*Rad*	*WF*	*gw*
77	an35	*mc*	*F*	*Adt*	*Fem*	*NZ*	*pa*
78	bdeer9	*bd*	*F*	*Adt*	*Fem*	*TZ*	*pa*
79	beruk48	*ptm*	*M*	*Adt*	*Fem*	*MZ*	*pa*
80	beruk55	*ptm*	*M*	*Adt*	*Fem*	*MZ*	*pa*
81	beruk67	*ptm*	*M*	*Adt*	*Tib*	*MZ*	*pa*
82	bintrg28	bearcat	*F*	*Adt*	*Fem*	*MZ*	*pa*
833	bintrg32	bearcat	*F*	*Adt*	*Tib*	*MZ*	*pa*
84	blm12	*blm*	*M*	*Adt*	*Fem*	*NZ*	*pa*
85	bone02	*mc*	*M*	*Adt*	*Fem*	*NZ*	*pa*
86	c10	cow	*?*	*Adt*	*Fem*	*But*	*sl*
87	c13	cow	*?*	*Adt*	*Fem*	*But*	*sl*
88	c17	cow	*?*	*Adt*	*Fem*	*But*	*sl*
89	c20	cow	*?*	*Adt*	*Fem*	*But*	*sl*
90	gmd130	*gm*	*F*	*Adt*	*Fem*	*NZ*	*pa*
91	gmdc	*gm*	*?*	*Adt*	*Fem*	*NZ*	*pa*
92	goat127	goat	*?*	*Adt*	*Fem*	*But*	*sl*
93	L7	cow	*?*	*Adt*	*Rad*	*Farm*	*sl*
94	c19	cow	*?*	*Adt*	*Fem*	*But*	*sl*
95	goatb	goat	*?*	*Adt*	*Fem*	*But*	*sl*
96	hkmbg64	*bp*	*M*	*Adt*	*Tib*	*MZ*	*pa*
97	hkmbg65	*bp*	*M*	*Adt*	*Fem*	*MZ*	*pa*
98	hkmbg52	*bp*	*M*	*Adt*	*Hum*	*MZ*	*pa*
99	hmbg62	*bp*	*M*	*Adt*	*Rad*	*MZ*	*pa*
100	k1	buffalo	*?*	*Adt*	*Rad*	*Farm*	*sl*
101	kcgbatu30	*lc*	*M*	*Adt*	*Fem*	*MZ*	*pa*
102	kmbg41	serow	*F*	*Adt*	*Tib*	*MZ*	*pa*
103	kmbgg26	serow	*F*	*Adt*	*Fem*	*MZ*	*pa*
104	kongkang47	*sl*	*M*	*Adt*	*Rad*	*MZ*	*pa*
105	kucingb37	*lc*	*M*	*Adt*	*Tib*	*MZ*	*pa*
106	kucingb50	*lc*	*M*	*Adt*	*Fem*	*MZ*	*pa*
107	kucingb51	*lc*	*M*	*Adt*	*Tib*	*MZ*	*pa*
108	kucingh42	*fhc*	*M*	*Adt*	*Fem*	*MZ*	*pa*
109	L2	cow	*?*	*Adt*	*Rad*	*Farm*	*sl*
110	L9	cow	*?*	*Adt*	*Rad*	*Farm*	*sl*
111	musangj39	*lic*	*M*	*Adt*	*Rad*	*MZ*	*pa*
112	musangj49	*lic*	*M*	*Adt*	*Tib*	*MZ*	*pa*
113	musangp18	*cpc*	*F*	*Adt*	*Fem*	*MZ*	*pa*
114	pygonyh	*ph*	*?*	*Adt*	*Fem*	*NZ*	*pa*
115	sheep116	sheep	*?*	*Adt*	*Rad*	*But*	*sl*
116	sheep131	sheep	*?*	*Adt*	*Fem*	*But*	*sl*

117	sheep132	sheep	*?*	*Adt*	*Tib*	*But*	*sl*
118	sheep138	sheep	*?*	*Adt*	*Fem*	*But*	*sl*
119	slmonkey129	*slm*	*F*	*Adt*	*Fem*	*NZ*	*pa*
120	deer32	deer	*?*	*Adt*	*Rad*	*NZ*	*pa*
121	leopardcat	*lc*	*?*	*Adt*	*Fem*	*NZ*	*pa*
122	leopcat38	*lc*	*M*	*Adt*	*Hum*	*NZ*	*pa*
123	ltmacaque	*ltm*	*?*	*Adt*	*Fem*	*NZ*	*pa*
124	mjebat61	*lic*	*M*	*Adt*	*Fem*	*NZ*	*pa*
125	msedeerzn	*md*	*M*	*Adt*	*Fem*	*NZ*	*pa*
126	ptmacaq54	*ptm*	*M*	*Adt*	*Tib*	*NZ*	*pa*
127	whgibbon	*whg*	*?*	*Adt*	*Fem*	*NZ*	*pa*
128	musangp46	*cpc*	*M*	*Adt*	*Hum*	*NZ*	*pa*
129	rabbit23	rabbit	*M*	*Adt*	*Hum*	*OF*	*pa*

Appendix 3 Human Sample Analysis

Table 36 The difference between known and estimated age in male and female bone thin section.

Male (n = 50)			Female (n = 14)		
Known age	Estimated age	Difference in age	Known age	Estimated age	Difference in age
38	38.65	0.65	38	30.21	-7.79
37	49.67	12.67	29	31.77	2.77
41	39	-2	22	29.78	7.78
28	30.77	2.77	32	34.15	2.15
39	38.16	-0.84	29	33.73	4.73
78	49.52	-28.48	29	47.61	18.61
46	38.65	-7.35	90	50.43	-39.57
37	40.04	3.04	91	46.71	-44.29
56	43.29	-12.71	40	37.62	-2.38
52	45.51	-6.49	76	62.03	-13.97
42	44.66	2.66	31	31.17	0.17
39	40.81	1.81	25	49.35	24.35
39	38.75	-0.25	48	41.07	-6.93
52	51.94	-0.06	22	34.12	12.12
21	49.98	28.98			
42	43.23	1.23			
52	53.26	1.26			
33	33.33	0.33			
38	46.61	8.61			
50	41.83	-8.17			
32	41.46	9.46			
47	42.02	-4.98			
35	36.52	1.52			
48	40.01	-7.99			
26	25.42	-0.58			
22	33.55	11.55			
40	43.86	3.86			
63	48.79	-14.21			
47	36.98	-10.02			
67	48.58	-18.42			
52	46.04	-5.96			
50	48.08	-1.92			
64	57.17	-6.83			
49	35.38	-13.62			
29	38.3	9.3			
27	35.64	8.64			
40	24.11	-15.89			
53	32.98	-20.02			
33	35.6	2.6			
32	31.18	-0.82			
34	44.53	10.53			
38	37.54	-0.46			
25	40.62	15.62			
53	49.46	-3.54			

31	32.84	1.84
33	38.41	5.41
32	33.54	1.54
37	43.05	6.05
45	38.83	-6.17
40	41.62	1.62

Appendix 4 Research Instruments

1.	Calipers	Absolute Digimatic, Japan.
2.	Saw Microtome	*LEICA SP* 1600, Germany.
3.	Grinder/Polisher	Phoenix Beta Buehler, Dusseldorf.
4.	Grinding paper	Diameter 200 mm, 600 Grit (Cat. No. 30- 5218-600, Buehler, Germany).
5.	Polishing cloth	White felt, diameter 200 mm (Bestell-Nr.: 16 20 02, Buehler, Dusseldorf).
6.	Image analyser	*SIS* Soft Imaging System 3.2 Software Package, Europe.
7.	Transmitted light microscope	Olympus *BX51M*, Japan.
8.	Camera	Digital Camera, Olympus *DP* 70, Japan.
9.	Objective micrometre	*OB-M*, 0.01 mm, 1/100, *AX0001*, Olympus, Japan.
10.	Di-ethyl ether	Lab. grade: *Cat. No D/2500/PB17*, Fischer Scientific Int. Co., *UK*.
11.	Resin	Buehler epo-thin low viscosity (*Cat. No*: 20-8140-032, *USA*).
12.	Hardener	Buehler epo-thin epoxy hardener (*Cat. No*: 20-8142-016, *USA*).

Appendix 5 Documents

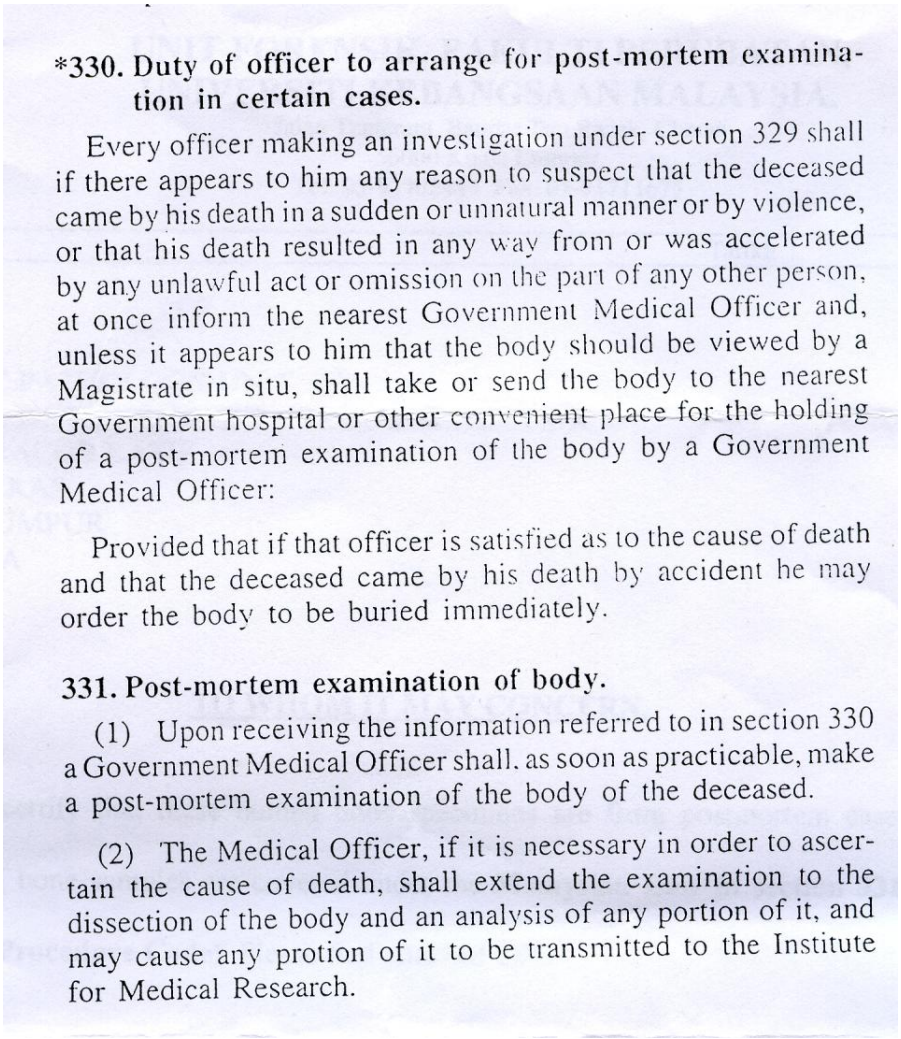

***330. Duty of officer to arrange for post-mortem examination in certain cases.**

Every officer making an investigation under section 329 shall if there appears to him any reason to suspect that the deceased came by his death in a sudden or unnatural manner or by violence, or that his death resulted in any way from or was accelerated by any unlawful act or omission on the part of any other person, at once inform the nearest Government Medical Officer and, unless it appears to him that the body should be viewed by a Magistrate in situ, shall take or send the body to the nearest Government hospital or other convenient place for the holding of a post-mortem examination of the body by a Government Medical Officer:

Provided that if that officer is satisfied as to the cause of death and that the deceased came by his death by accident he may order the body to be buried immediately.

331. Post-mortem examination of body.

(1) Upon receiving the information referred to in section 330 a Government Medical Officer shall, as soon as practicable, make a post-mortem examination of the body of the deceased.

(2) The Medical Officer, if it is necessary in order to ascertain the cause of death, shall extend the examination to the dissection of the body and an analysis of any portion of it, and may cause any protion of it to be transmitted to the Institute for Medical Research.

Figure 21 Criminal procedure code (*CPC* 331 s.2), which authorises the retention of body tissues for analysis in autopsy.

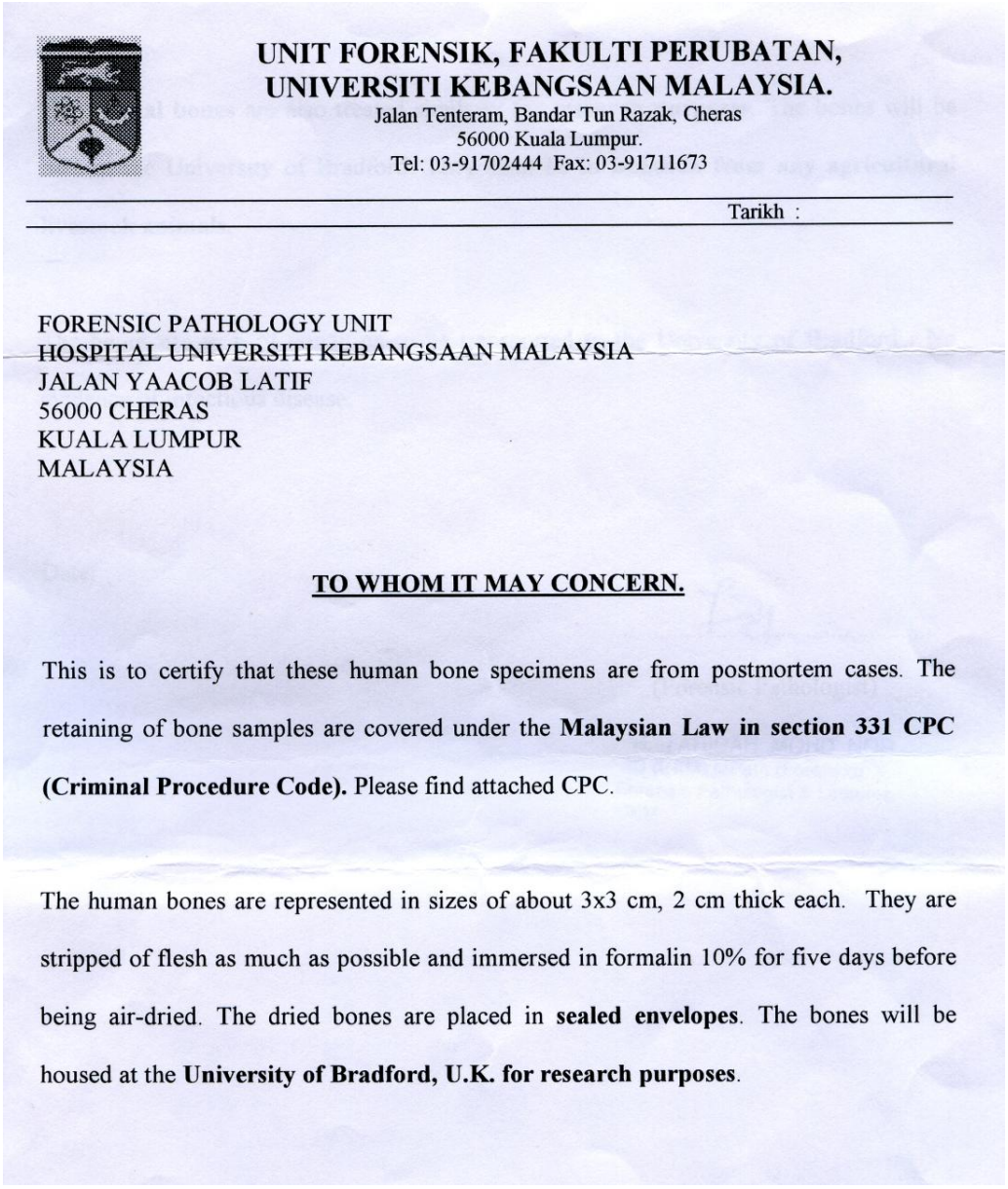

UNIT FORENSIK, FAKULTI PERUBATAN,
UNIVERSITI KEBANGSAAN MALAYSIA.
Jalan Tenteram, Bandar Tun Razak, Cheras
56000 Kuala Lumpur.
Tel: 03-91702444 Fax: 03-91711673

Tarikh :

FORENSIC PATHOLOGY UNIT
HOSPITAL UNIVERSITI KEBANGSAAN MALAYSIA
JALAN YAACOB LATIF
56000 CHERAS
KUALA LUMPUR
MALAYSIA

TO WHOM IT MAY CONCERN.

This is to certify that these human bone specimens are from postmortem cases. The retaining of bone samples are covered under the **Malaysian Law in section 331 CPC (Criminal Procedure Code).** Please find attached CPC.

The human bones are represented in sizes of about 3x3 cm, 2 cm thick each. They are stripped of flesh as much as possible and immersed in formalin 10% for five days before being air-dried. The dried bones are placed in **sealed envelopes**. The bones will be housed at the **University of Bradford, U.K. for research purposes**.

Figure 22 A medical document for certification of bone samples to be transfered to the University of Bradford for research purposes.

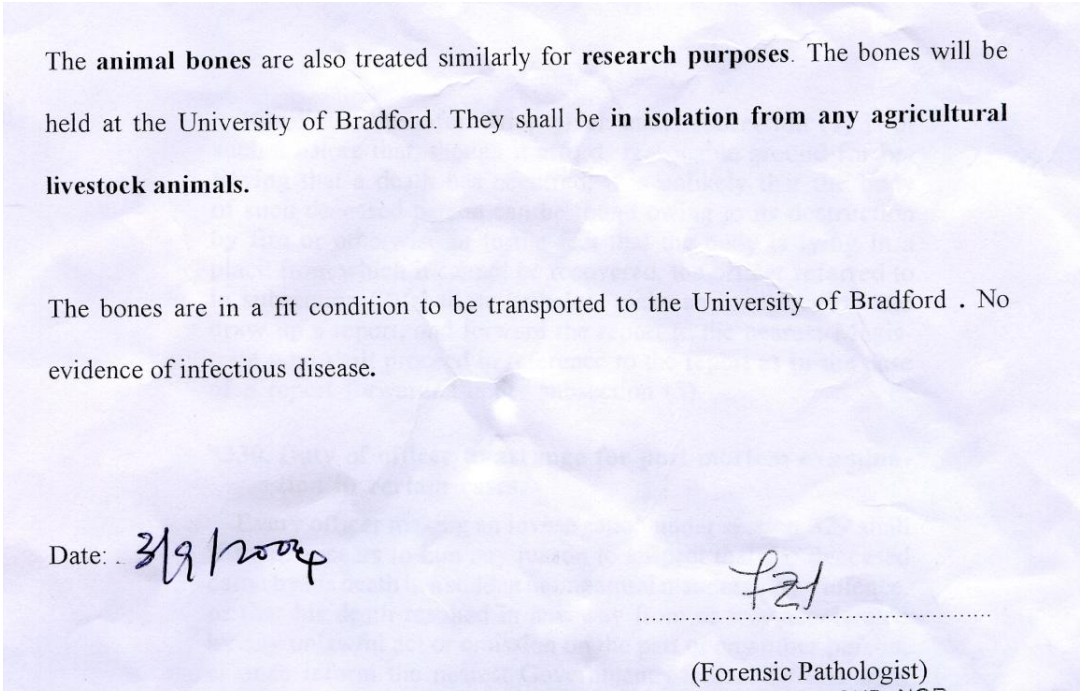

The **animal bones** are also treated similarly for **research purposes**. The bones will be held at the University of Bradford. They shall be **in isolation from any agricultural livestock animals.**

The bones are in a fit condition to be transported to the University of Bradford . No evidence of infectious disease.

Date: 3/9/2004

(Forensic Pathologist)

(Continued from Figure 22)

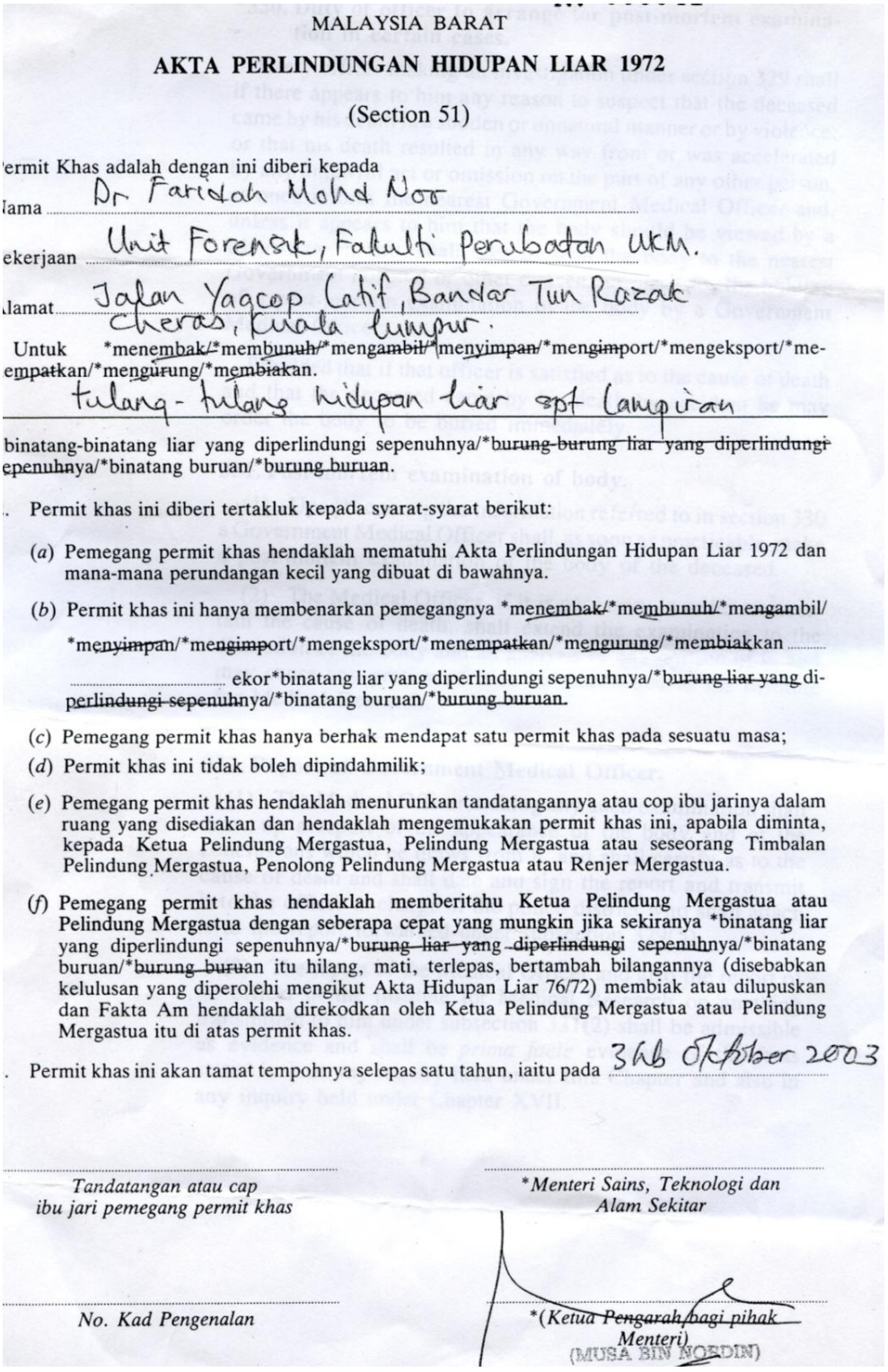

MALAYSIA BARAT

AKTA PERLINDUNGAN HIDUPAN LIAR 1972

(Section 51)

'ermit Khas adalah dengan ini diberi kepada

lama Dr Faridah Mohd Noor

ekerjaan Unit Forensik, Fakulti Perubatan UKM.

lamat Jalan Yaacop Latif, Bandar Tun Razak Cheras, Kuala Lumpur.

Untuk *menembak/*membunuh/*mengambil/*menyimpan/*mengimport/*mengeksport/*me-empatkan/*mengurung/*membiakan.

tulang-tulang hidupan liar spt Lampiran

binatang-binatang liar yang diperlindungi sepenuhnya/*~~burung-burung liar yang diperlindungi~~ sepenuhnya/*binatang buruan/*~~burung buruan~~.

. Permit khas ini diberi tertakluk kepada syarat-syarat berikut:

(*a*) Pemegang permit khas hendaklah mematuhi Akta Perlindungan Hidupan Liar 1972 dan mana-mana perundangan kecil yang dibuat di bawahnya.

(*b*) Permit khas ini hanya membenarkan pemegangnya *~~menembak/~~*membunuh/*mengambil/ *~~menyimpan~~/*~~mengimport~~/*mengeksport/*~~menempatkan~~/*mengurung/*membiakkan ..... ekor*binatang liar yang diperlindungi sepenuhnya/*~~burung liar yang diperlindungi sepenuhnya~~/*binatang buruan/*~~burung buruan~~.

(*c*) Pemegang permit khas hanya berhak mendapat satu permit khas pada sesuatu masa;

(*d*) Permit khas ini tidak boleh dipindahmilik;

(*e*) Pemegang permit khas hendaklah menurunkan tandatangannya atau cop ibu jarinya dalam ruang yang disediakan dan hendaklah mengemukakan permit khas ini, apabila diminta, kepada Ketua Pelindung Mergastua, Pelindung Mergastua atau seseorang Timbalan Pelindung Mergastua, Penolong Pelindung Mergastua atau Renjer Mergastua.

(*f*) Pemegang permit khas hendaklah memberitahu Ketua Pelindung Mergastua atau Pelindung Mergastua dengan seberapa cepat yang mungkin jika sekiranya *binatang liar yang diperlindungi sepenuhnya/*~~burung liar yang diperlindungi~~ sepenuhnya/*binatang buruan/*~~burung buru~~an itu hilang, mati, terlepas, bertambah bilangannya (disebabkan kelulusan yang diperolehi mengikut Akta Hidupan Liar 76/72) membiak atau dilupuskan dan Fakta Am hendaklah direkodkan oleh Ketua Pelindung Mergastua atau Pelindung Mergastua itu di atas permit khas.

. Permit khas ini akan tamat tempohnya selepas satu tahun, iaitu pada 3hb Oktober 2003

Tandatangan atau cap ibu jari pemegang permit khas

No. Kad Pengenalan

**Menteri Sains, Teknologi dan Alam Sekitar*

**(Ketua Pengarah bagi pihak Menteri)*

(MUSA BIN NORDIN)

Figure 23 The permit from the 'Ministry of Wild Life' authorising export of bone overseas for research purposes.